LAMINAR BOUNDARY LAYER SEPARATION AND NEAR WAKE FLOW FOR A SMOOTH BLUNT BODY AT SUPERSONIC AND HYPERSONIC SPEEDS

Thesis by

Jean-Marie Grange

In Partial Fulfillment of the Requirements

For the Degree of

Aeronautical Engineer

California Institute of Technology

Pasadena, California

1966

(Submitted May 26, 1966)

ACKNOWLEDGMENTS

The author expresses his appreciation to Mr. John Klineberg and Professor Lester Lees for their guidance, help and encouragement throughout the course of this investigation. He would also like to thank Mr. Denny Ko and Mr. Irwin Alber for assistance in checking the basic equations and computations.

This research was sponsored by the U. S. Air Force Office of Scientific Research under Contract No. AF 49(638)-1298.

ABSTRACT

At supersonic and hypersonic speeds the location of the boundary layer separation point on the surface of a smooth, blunt body is not fixed á priori, but is determined by the pressure rise communicated upstream through the subcritical base flow. By utilizing the integral or moment method of Reeves and Lees the separation-interaction region is joined smoothly to the near-wake interaction region passing through a "throat" downstream of the rear stagnation point. One interesting feature of this problem is that the viscous flow over the blunt body "overexpands" and goes supercritical. This flow is joined to the near-wake by means of a supercritical-subcritical "jump" upstream of separation, and the jump location is determined by the matching conditions.

Downstream of the jump the viscous flow separates in response to the pressure rise, and forms a constant pressure mixing region leading into the near wake. As an illustrative example the method is applied to an adiabatic circular cylinder at $M_o = 6$, and the results are compared with the experimental measurements of Dewey and McCarthy. This method can be extended to non-adiabatic bodies, and to slender bodies with smooth bases, provided that the radius of curvature is large compared to the boundary layer thickness.

TABLE OF CONTENTS

LIST OF FIGURES

LIST OF SYMBOLS

a	velocity profile parameter; also speed of sound
B	$\mathcal{H} + \left(\frac{1+m_e}{m_e}\right)(1-\tilde{e})$
c_v, c_p	specific heat at constant volume and constant pressure, respectively
C	$\left(\frac{\mu}{\mu_\infty}\right)/\left(\frac{T}{T_\infty}\right)$
d_1	height of edge of viscous layer above wake axis at the beginning of pressure plateau (Fig. 1)
d	cylinder diameter
$D(M_e, a)$	function defined in Eq. (9)
$\tilde{e}$	$-\frac{1}{\delta_i^*}\int_0^{\delta_i} S\,dY$
f	function defined in Eq. (4b)
G	$\int_0^{\delta} \rho u^3\,dy$, twice the flux of mechanical energy
h	static enthalpy; also function defined in Eq. (4c)
h_s	total enthalpy
$\mathcal{H}$	θ_i/δ_i^*
J	θ_i^*/δ_i^*
K	$\int_0^{\delta} u\,dy$
m	$\frac{\gamma-1}{2} M^2$
M	Mach number
N_1, N_2, N_3	functions defined in Eq. (9)
p	static pressure
P	$\frac{\delta_i^*}{U_e}\left(\frac{\partial U}{\partial Y}\right)_{Y=0}$, surface shear stress function

LIST OF SYMBOLS (Cont'd)

Q	$- \delta_i^* \left[\frac{\partial}{\partial Y}\left(S/S_w\right)\right]_{Y=0}$
R	$\frac{2\delta_i^*}{U_e^2} \int_0^{\delta_i} \left(\frac{\partial U}{\partial Y}\right)^2 dY$
$Re_{\infty, d}$	$\frac{a_\infty}{\nu_\infty} M_\infty d$
$\widetilde{R}e_{\delta_i^*}$	$\frac{a_\infty}{\nu_\infty} M_e \delta_i^*$
$Re_{o, d}$	$\frac{u_o d}{\nu_o}$
REINF	$\frac{u_\infty d}{\nu_\infty}$
	(the four quantities above: Reynolds Numbers)
S	$\left(\frac{h_s}{h_{s_e}} - 1\right)$, total enthalpy function
T*	$\frac{1}{\delta_i^*} \int_0^{\delta_i} \frac{U}{U_e} \frac{S}{S_w} dy$, enthalpy flux function
u, v	velocity components parallel and normal to surface, respectively
u*	$\left(\frac{U}{U_e}\right)_{\psi=0}$, normalized velocity component along dividing streamline
U	$u\left(\frac{a_\infty}{a_e}\right)$, Stewartson's transformed velocity
x, y	Stewartson's transformed coordinates
Z	$\frac{1}{\delta_i^*} \int_0^{\delta_i} \left(\frac{U}{U_e}\right) dy$

$\alpha(x)$	inclination of local tangent to surface, measured positive clockwise with respect to surface inclination at reference point x_o
β	Falkner Skan pressure gradient parameter; also $\frac{p_e a_e}{p_\infty a_\infty}$
γ	c_p/c_v , ratio of specific heats
δ	boundary layer thickness
δ_i	transformed boundary layer thickness
δ_i^*	$\int_o^{\delta_i} \left(1 - \frac{U}{U_e}\right) dy$, transformed boundary layer displacement thickness
δ_R^*	$\left(\frac{a_\infty}{\nu_\infty} M_\infty r\right) \left(\frac{\delta_i^*}{r}\right)^2$
$\theta \equiv \theta_i$	$\int_o^{\delta_i} \frac{U}{U_e} \left(1 - \frac{U}{U_e}\right) dY$, boundary layer momentum thickness
θ_i^*	$\int_o^{\delta_i} \frac{U}{U_e} \left(1 - \frac{U^2}{U_e^2}\right) dY$, transformed mechanical energy thickness
Ⓗ	local angle between "external" streamline at $y = \delta$ and the x-axis, $\tan^{-1}\left(\frac{v_e}{u_e}\right)$
μ	viscosity
ν	Prandtl-Meyer angle; also kinematic viscosity, μ/ρ
ρ	gas density
ψ	stream function

Subscripts

B	Blasius
CL	centerline
CR	critical
e	local "external" inviscid
i	transformed
r. s. p.	rear stagnation point
o	free stream ahead of bow shock
p. p.	pressure plateau
w	wall (surface)
∞	neck conditions

I. INTRODUCTION

Our understanding of the flow in the near-wake behind smooth, blunt bodies at supersonic and hypersonic speeds has advanced considerably as a result of the experimental studies of Dewey[1] and McCarthy and Kubota[2], and the theoretical analysis of Reeves and Lees[3]. The key to the solution of this problem is the strong interaction between the viscous flow originating in the boundary layer and free shear layer, and the "external" inviscid flow (Fig. 1). Unlike the situation in ordinary boundary layer theory the pressure distribution along the wake axis is not known á priori, but must be obtained as part of the solution. Viscous-inviscid interaction occurs through the pressure field generated by the induced streamline deflection at the outer edge of the viscous layer. According to this "model" the compression along the wake axis is a smooth process rather than the sudden compression assumed by Chapman[4] and others. In fact for laminar flow the length of the compression region upstream of the rear stagnation point is still about 1.5 body diameters at Reynolds numbers of the order of 10^6, and nearly half of the static pressure rise occurs downstream of the rear stagnation point (Ref. 3).

Because of the complexity of the problem, including regions of reversed-flow, Reeves and Lees[3, 5] employ an integral or moment method to describe the viscous flow. In addition to the usual momentum integral they utilize the first moment of momentum (mechanical energy). When these two equations are combined with the continuity equation and the Prandtl-Meyer relation connecting pressure and streamline inclination in the inviscid flow, one has a complete set of three equations for the three parameters $\delta_i^*(x)$, $M_e(x)$ and an independent velocity profile parameter a(x) (for adiabatic flow). As shown originally by Crocco[6] and Lees a formulation of the viscous-inviscid interaction of this kind leads to the conclusion that the near-wake flow is "subcritical" at the rear stagnation point, but passes through a "throat" into the supercritical region somewhere downstream of the rear stagnation point. At a given Mach number and Reynolds number the base pressure or flow angle is uniquely determined by the requirement that the correct solution must pass smoothly through the throat. In this sense the situation is analogous to the inviscid choked flow in a converging-diverging nozzle. In fact Crocco[7] has shown that in a subcritical flow pressure disturbances are felt upstream, while in a supercritical flow the adjustment to a pressure change can occur only across a supercritical-subcritical "jump", or "shock".[8]

In order to obtain a complete solution to the base flow problem for a blunt body, the near wake interaction region must be joined to the boundary layer separation-interaction region on the body. Since Reeves and Lees[3] were concentrating mainly on the near-wake interaction zone behind a circular cylinder, they assumed that the separation point is held fixed at a location 125° around the body from the forward stagnation point. By using standard methods the boundary layer growth up to this fixed point is calculated on the basis of a known (experimental) static pressure distribution. Reeves and Lees assume that the velocity profile jumps to the separation-point profile instantaneously across a discontinuity at this location. Since only a small pressure rise is required to separate a laminar boundary layer, they take the "external" Mach number M_e as constant across the "jump". By using mass conservation all quantities just downstream of the jump are determined, and these values furnish the initial conditions for the constant pressure mixing region downstream of separation. No attempt was made to match the shear layer angle to the induced angle $\Theta(\delta)$ of the boundary layer at separation. With the location of the separation point arbitrarily fixed there are only three unknowns for a given free stream Mach number and Reynolds number $Re_{o,d}$: (1) length of the constant pressure mixing region; (2) length of the wake interaction region or compression zone upstream of the rear stagnation point; (3) value of δ_i^* at the rear stagnation point. Reeves and Lees[3] join the constant pressure mixing solution to the near wake interaction solution by matching M_e [or Θ], u^*, and the mass flow above the zero velocity line.

Actually the location of the separation point on the body surface is not fixed á priori, but moves in response to the pressure rise communicated upstream through the subcritical base flow. A "jump" is required, as we shall see, in order to connect the supercritical viscous flow over the body with the initially subcritical wake flow, but the velocity profile just downstream of the jump is not a separation-point profile. To this extent the work of Reeves and Lees is incomplete. The main purpose of the present study is to treat the separation-interaction region more carefully, and then to join this region smoothly to the constant pressure mixing region and near-wake interaction zone.

The actual numerical example chosen is the same case of an adiabatic circular cylinder at a freestream Mach number of 6 treated by Reeves and Lees[3]. In Section 2 the basic differential equations of the Lees-Reeves method are written down for adiabatic flow, except that the curvature of the solid surface is now taken into account in the Prandtl-Meyer relation. These equations are first applied to the calculation of the boundary layer around the cylinder for a given experimental static pressure distribution.

If one tries to calculate the subsequent development of the viscous layer including interaction starting from some arbitrary point on the surface, one finds that the flow goes supercritical at a point about 97° around the cylinder from the forward stagnation point. But the flow in the near-wake is initially subcritical. Thus a jump is required somewhere aft of $\theta = 97°$. In Section 3 the laminar supercritical-subcritical jump conditions are derived for both adiabatic and non-adiabatic flow, and in Section 4 the equations for the now subcritical viscous layer downstream of the jump are integrated through the separation point and into the constant pressure mixing region. Section 5 deals with the near-wake interaction region in the manner established by Reeves and Lees[3], and this zone is joined smoothly to the constant pressure mixing region. Finally, in Section 6 a typical complete solution for the adiabatic circular cylinder is worked out, and possible extensions of this method are briefly discussed.

II. DIFFERENTIAL EQUATIONS: APPLICATION TO FLOW AROUND AN ADIABATIC CIRCULAR CYLINDER FROM THE FORWARD STAGNATION POINT TO THE JUMP LOCATION

As shown by Lees and Reeves[5] the well-known integral or moment method can be successfully utilized to describe interacting separated and reattaching flows, as well as attached flows, provided the velocity profiles employed as weighting functions have the qualitatively correct behavior. For flows near a solid surface the Stewartson[9] solutions of the Falkner-Skan equations are shown to be the simplest appropriate family, including the branch corresponding to reversed-flow profiles. For wake flows another set of solutions of the Falkner-Skan equations with zero shear stress on the axis, also found by Stewartson[9], is the simplest appropriate family. In every case it is essential to "unhook" the profiles from the pressure gradient parameter, β, and to describe them in terms of an independent profile parameter a(x), or $\mathcal{H}(x)$, that is not uniquely related to the local pressure gradient.

For <u>adiabatic flow</u> the three independent parameters of the problem are $M_e(x)$, a(x) or $\mathcal{H}(x)$, and $\delta_i^*(x)$. The "history" of these three parameters is determined by three first order non-linear, ordinary differential equations, as follows:[3, 5]

<u>CONTINUITY</u>

$$B \frac{d\delta_i^*}{dx} + \delta_i^* \frac{d\mathcal{H}}{da} \frac{da}{dx} + f \frac{\delta_i^*}{M_e} \frac{dM_e}{dx} = \frac{\beta C h}{\widetilde{R}e_{\delta_i^*}} \tag{1}$$

MOMENTUM

$$\mathcal{K} \frac{d\delta_i^*}{dx} + \delta_i^* \frac{d\mathcal{K}}{da} \frac{da}{dx} + (2\mathcal{K}+1) \frac{\delta_i^*}{M_e} \frac{dM_e}{dx} = \frac{\beta C P}{\widetilde{R}e_{\delta_i^*}} \tag{2}$$

MOMENT OF MOMENTUM (MECHANICAL ENERGY)

$$J \frac{d\delta_i^*}{dx} + \delta_i^* \frac{dJ}{d\mathcal{K}} \frac{d\mathcal{K}}{da} \frac{da}{dx} + 3J \frac{\delta_i^*}{M_e} \frac{dM_e}{dx} = \frac{\beta C R}{\widetilde{R}e_{\delta_i^*}} \tag{3}$$

where

$$B = \mathcal{K} + \frac{1+m_e}{m_e} \tag{4a}$$

$$f = \left(2 + \frac{\gamma+1}{\gamma-1} \frac{m_e}{1+m_e}\right)\mathcal{K} + \left(\frac{3\gamma-1}{\gamma-1}\right) + \frac{M_e^2-1}{m_e(1+m_e)} \quad Z \tag{4b}$$

$$h = \widetilde{R}e_{\delta_i^*} \frac{(1+m_e)}{m_e(1+m_\infty)} \tan Ⓗ \tag{4c}$$

$$\widetilde{R}e_{\delta_i^*} = \frac{a_\infty}{\nu_\infty} M_e \delta_i^* \tag{4e}$$

$$C = \left(\mu/\mu_\infty\right)/\left(T/T_\infty\right) \quad \text{and} \quad \beta = \frac{p_e a_e}{p_\infty a_\infty} \tag{4f}$$

and the other quantities are defined in References (3) and (5) and in the List of Symbols.

For attached flow the independent parameter a(x) is given by the relation

$$a(x) = \left.\frac{\partial\left(U/U_e\right)}{\partial\left(Y/\delta_i\right)}\right|_{Y=0}$$

while for separated flows near a solid surface

$$a(x) = \left[Y/\delta_i\right]_{U/U_e=0}$$

In wake flows upstream of the rear stagnation point[3],

$$a(x) = U^* = \frac{U_{\psi=o}}{U_e} \quad ,$$

and $$a(x) = \frac{U_{\mathbb{C}}}{U_e}$$

downstream of the rear stagnation point.

In these viscous-inviscid interactions the "external" inviscid flow $M_e(x)$ cannot be specified á priori, but is determined by the induced inclination Ⓗ of the streamline at the outer edge of the boundary layer, given by Eq. (1). For many flows the Prandtl-Meyer relation connecting Ⓗ with M_e is a good approximation, except that the curvature of the surface must also be taken into account. Thus

$$\nu(x) - \nu(x_o) = -\alpha(x) - Ⓗ(x) , \tag{5}$$

where $\nu(x_o)$ is evaluated at some reference station, and $\alpha(x)$ is the inclination of the local tangent to the surface, measured positive clockwise with respect to the surface inclination at x_o. With the aid of this relation [Eq. (5)], Eqs. (1)-(3) completely determine the interaction.

John Klineberg obtained additional solutions of the Cohen-Reshotko[10] or Stewartson[9] equations both for adiabatic flow and for the "highly-cooled" case of $S_w = -0.8$. By using these solutions he was able to evaluate the quantities, $\mathcal{X}$, J, Z, R, P and the derivative $\frac{dJ}{d\mathcal{X}}$ appearing in Eq. (1)-(3) quite accurately. He then curve-fitted these functions as polynomials in "a". These functions are plotted in Figures 2-7, and the coefficients of the polynomials are given in Tables 1 and 2. $\left[\text{For example, } \mathcal{X} = \sum_{k=o}^{7} C_k a^k\right]$

By regarding Eqs. (1)-(3) as algebraic equations for the three unknown first derivatives of δ_i^*, M_e and a, and solving simultaneously, one obtains the following equations for adiabatic flow:

$$\frac{\delta_i^*}{M_e} \frac{dM_e}{dx} = \frac{C}{\mathcal{R}e_{\delta_i^*}} \frac{N_1(M_e, a, h)}{D(M_e, a)} \tag{6}$$

$$\delta_i^* \frac{d\mathcal{X}}{dx} = \frac{C}{\mathcal{R}e_{\delta_i^*}} \frac{N_2(M_e, a, h)}{D(M_e, a)} \tag{7}$$

$$\frac{d\delta_i^*}{dx} = \frac{C}{\mathcal{R}e_{\delta_i^*}} \frac{N_3(M_e, a, h)}{D(M_e, a)} \tag{8}$$

where $N_1(M_e, a, h) = \left(J - \mathcal{X}\frac{dJ}{d\mathcal{X}}\right) h + (\mathcal{X}R - PJ) + \left(P\frac{dJ}{d\mathcal{X}} - R\right) B$

$$N_2(M_e, a, h) = J(\mathcal{X}-1)h + (PJ - \mathcal{X}R)f + [(2\mathcal{X}+1)R - 3JP]\, B$$

$$N_3(M_e, a, h) = \left[(2\mathcal{X}+1)\frac{dJ}{d\mathcal{X}} - 3J\right] h + \left(R - P\frac{dJ}{d\mathcal{X}}\right) f + \left[3JP - (2\mathcal{X}+1)R\right] \tag{9}$$

$$D(M_e, a) = \left(J - \mathcal{X}\frac{dJ}{d\mathcal{X}}\right) f + (\mathcal{X}-1)\, J + \left[(2\mathcal{X}+1)\frac{dJ}{d\mathcal{X}} - 3J\right] B$$

As shown by Lees and Reeves[5] the point D = 0 is a singular point of this system of equations. If N_j vanishes when D = 0 (j = 1,2 or 3) then the other two N's also vanish and this point is a "saddle-point" or "throat" marking the transition between "subcritical" and "supercritical" flow. In fact the situation is similar to the subsonic-supersonic transition in a converging-diverging nozzle. If $N_j \neq 0$ this point is a turning point and the integral curve is thrown back. Physically, a subcritical flow is capable of generating its own self-induced disturbance interacting with the "external" supersonic flow in response to a downstream event. A supercritical flow, on the other hand, cannot "feel" disturbances originating downstream. Thus the transition from a supercritical flow to a subcritical flow must occur across a "jump" or "shock" somewhat analogous to the normal shock in the diverging portion of a supersonic nozzle.

For adiabatic flow the locus of critical points $D = 0$ is a unique function of a and M_e (Fig. 8). We see that the Blasius flow is always subcritical and the singularity $D = 0$ always lies in the range $a > a_B$, corresponding to a flow with a negative pressure gradient of a certain strength, or a falling pressure applied over a sufficient length in the flow direction. The flow around a circular cylinder (or other blunt body) at supersonic speeds is an interesting example of a case in which the boundary layer goes supercritical. Of course the viscous layer is always subcritical in the subsonic portion of the inviscid flow near the front stagnation point. Downstream of the sonic point, however, the value of a_{CR} rapidly decreases with increasing M_e (Fig. 8), while a(x) grows because of the action of the negative pressure gradient in "filling out" the velocity profiles. If $D = 0$ at some point on the body then N_1, N_2 and N_3 must vanish there also if the solution is to be continued downstream. This requirement leads to a unique value of h at the critical point, namely,

$$\widetilde{R}e_{\delta_i^*} \tan \text{Ⓗ} = C(1+m_\infty)\left[F(a) + \frac{m_e}{1+m_e} P\right] \tag{10}$$

where, for adiabatic flow,

$$F(a) = \left(P \frac{dJ}{d\mathcal{H}} - R\right) \Big/ \left(\mathcal{H} \frac{dJ}{d\mathcal{H}} - J\right) \tag{10a}$$

It turns out that F(a) and P(a) are both > 0 for $a \geq a_B$; hence Ⓗ > 0 at the critical point, and this situation is entirely possible when the flow expands because of surface curvature.

Strictly speaking the development of the boundary layer starting at the forward stagnation point should be calculated taking into account the interaction with the external flow. In the supersonic region, for example, such a calculation involves a coupling between the characteristics net and Eqs. (1)-(3). Since this problem is a formidable one in itself, and since the main interest in the present paper lies in the separation and wake phenomena, it was decided to adopt the procedure of Reeves and Lees[3] and regard $M_e(x)$ as given up to the "jump" location. The pressure distribution on the forward part of the cylinder was taken from McCarthy's[2] measurements, and the variations of M_e and $d(M_e)/d(x/r)$ were computed assuming isentropic flow around the cylinder. We can therefore drop the continuity equation [Eq. (1)] and consider only Eq. (2) and (3), which can be rewritten in terms of the variable $\delta_r{}^* = \left(\frac{a_\infty}{\nu_\infty} M_\infty r\right)\left(\frac{\delta_i{}^*}{r}\right)^2$ and solved for the derivatives $\frac{d\delta_r{}^*}{d(x/r)}$ and $\frac{da}{d(x/r}$, yielding,

$$\frac{d\delta_r{}^*}{d(x/r)} = \frac{\beta M_\infty \left(P \frac{dJ}{d\mathscr{H}} - R\right) + \left[3J - (2\mathscr{H}+1)\frac{dJ}{d\mathscr{H}}\right]\delta_r{}^* \frac{dM_e}{d(x/r)}}{\frac{M_e}{2}\left(\mathscr{H}\frac{dJ}{d\mathscr{H}} - J\right)} \tag{11}$$

$$\frac{da}{d(x/r)} = \frac{\beta M_\infty (R\mathscr{H} - PJ) + J(1-\mathscr{H})\,\delta_r{}^* \frac{dM_e}{d(x/r)}}{M_e \delta_r{}^* \frac{d\mathscr{H}}{da}\left(\mathscr{H}\frac{dJ}{d\mathscr{H}} - J\right)} \tag{12}$$

where $\beta^{-1} = \frac{p_\infty a_\infty}{p_e a_e} = \left(\frac{1+m_e}{1+m_\infty}\right)^{(3\gamma-1)/2(\gamma-1)}$

The initial conditions on $\delta_r{}^*$ and "a" are given by the conditions of boundedness on $\frac{d\delta_r{}^*}{d(x/r)}$ and $\frac{da}{d(x/r)}$ at the forward stagnation point, where $M_e = 0$ and $\frac{x}{r} = 0$. This condition requires that the numerators on the R.H.S. of Eq. (11) and (12) vanish. By eliminating $\delta_r{}^*$, we get the condition

$$3\,JP = R(2\mathcal{K} + 1)\ , \qquad \text{for which one obtains}$$

$$\left(\delta_r{}^*\right)_{stag.} = \frac{\beta\ M_\infty P}{(2\mathcal{K}+1)\,[dM_e/d(x/r)]_{x/r=0}}$$

Since $\left[\frac{dM_e}{d(x/r)}\right]_{x/r=0} = 1$, according to McCarthy's data, and $M_\infty = 2.5$ (neck Mach number for a free stream Mach number of 6.0), one finds:

$$a_{stag.} = 2.967$$

$$(\delta_r{}^*)_{stag.} = 26.97$$

One can show by a linearization of Eq. (11) and (12) around $a_{stag.}$ and $(\delta_r{}^*)_{stag.}$ that the stagnation point is a saddle point in the $(a - \delta_r{}^*)$ plane; therefore one has to start the integration of Eq. (11) and (12) by "kicking" the solution off the critical point by a small amount. The integration of these equations was performed on an IBM 7090 computer using a Runge-Kutta method started with Milne's method.

The distribution of a, $\delta_r{}^*$ and the normalized physical boundary layer thickness are shown in Fig. 9, where:

$$\frac{\delta}{r}\sqrt{\frac{a_\infty M_\infty}{\nu_\infty}} = \left(\frac{1+m_e}{1+m_\infty}\right)^{\frac{\gamma+1}{2\gamma-1}}\left[m_e(1+\mathcal{K}) + 1+Z\right]\sqrt{\delta_r{}^*} \qquad (13)$$

One can see that at $(x/r) = 1.20$, "a" exceeds the maximum value (3.90) obtained from the similar solutions of the Falkner-Skan equation in the adiabatic case, indicating that the method of local similarity fails downstream of that point and that the profiles are really non-similar. However, in order to continue the solution with this family of velocity profiles, it was assumed that "a" stays constant and equal to 3.9, and that all the integral functions keep their value at a = 3.9, which is to assume that the profiles take a constant shape for $\left(\frac{x}{r}\right) > 1.20$. Eq. (12) was then dropped and Eq. (11) integrated downstream of $x/_r = 1.20$; this equation becomes

$$\frac{d(\delta_i^*/r)}{d(x/r)} = \frac{1}{\mathscr{K}}\left[\beta \frac{P}{Re_{\delta_i^*}} - (2\mathscr{K}+1)\frac{\delta_i^*}{r}\frac{1}{M_e}\frac{dM_e}{d(x/r)}\right] \tag{14}$$

At $\left(\frac{x}{r}\right) = 1.2$, the outer flow is already supersonic and we calculate the angle of the streamline at the edge of the boundary layer with the wall, Ⓗ, from the continuity Eq. (1) rewritten as:

$$\tan Ⓗ = \left(\frac{1+m_e}{1+m_\infty}\right)^{\frac{\gamma+1}{2(\gamma-1)}} m_e \left\{B\frac{d(\delta_i^*/r)}{d(x/r)} + f\frac{\delta_i^*}{r}\frac{1}{M_e}\frac{dM_e}{d(x/r)}\right\} \tag{15}$$

because "a" is held constant.

Suppose now one tries to calculate the subsequent development of the viscous layer including interaction starting from some arbitrary point, at which the solution is assumed known from Eq. (11)-(15). Returning to the <u>full</u> equations [Eq. (1)-(3)] one finds that the viscous flow goes supercritical for $M_e = 2.4$ (Fig. 8) corresponding to $\frac{x}{r} = 1.69$ [a = 3.9]. But the wake flow is initially subcritical. In order to connect these two regions the flow must experience a sudden "jump" on the body surface from a supercritical to a subcritical state, followed by a smooth compression and flow separation leading into the near wake region.

III. LAMINAR SUPERCRITICAL-SUBCRITICAL JUMP CONDITIONS

In reality a supercritical flow has a high but finite "impedance" to the propagation of disturbances upstream through the subsonic portion of the boundary layer, so one expects the transition from supercritical to subcritical flow to occur over a few boundary layer thicknesses. However, within the framework of the present theory we regard this transition as discontinuous (Fig. 10), and allow for sudden "jumps" in the fluxes of mass, momentum and mechanical energy. The flow upstream of the jump is characterized by four quantities, namely M_e, δ_i^*, a(or $\mathcal{H}$) and T* (for non-adiabatic flow), and four jump conditions are required to determine the flow downstream of the jump uniquely. Three of these relations are derived from the known conservation laws for mass, momentum, and total enthalpy. In general the fourth quantity, namely the mechanical energy, or moment of momentum, is not a conservative quantity. In the limit of Δx_1 and Δx_2 both $\rightarrow 0$ (Fig. 10) the volume dissipation vanishes and we can write approximate jump conditions for this quantity as well. The jump conditions are written down for non-adiabatic flow, but the final relations are specialized to the case of adiabatic flow to fit in with the rest of this paper.

By referring to Fig. 10, one sees that as Δx_1 and $\Delta x_2 \rightarrow 0$ the effects of skin friction and heat transfer vanish, as well as the volume dissipation. Also the effect of the "external" streamline inclination drops out of the continuity equation.

With these observations the three jump conditions derived from the conservation laws are as follows:

MASS

$$\dot{m}_2 - \dot{m}_1 = (\rho_e u_e)_1 (\delta_2 - \delta_1) \tag{16}$$

MOMENTUM

$$I_2 - I_1 = (\rho_e u_e^2)_1 (\delta_2 - \delta_1) - \delta_2 (p_2 - p_1) \tag{17}$$

TOTAL ENTHALPY

$$\frac{M_{e_2}}{M_{e_1}} \frac{(\delta_i^*)_2}{(\delta_i^*)_1} \frac{T_2^*}{T_1^*} = 1 \tag{18}$$

where

$$\dot{m} = \int_0^\delta \rho u \, dy = \rho_\infty a_\infty M_e \delta_i^* Z \tag{19}$$

$$I = \int_0^\delta \rho u^2 dy = \rho_\infty a_\infty u_e M_e \delta_i^* (Z - \mathcal{X}) \tag{20}$$

and

$$\delta = \frac{a_\infty \rho_\infty}{a_e \rho_e} \delta_i^* (m_e B + Z) \tag{21}$$

where

$$B = \mathcal{X} + \left(\frac{1+m_e}{m_e}\right) (1 - \tilde{e})$$

The fourth jump condition, for mechanical energy or moment of momentum, is derived from the differential equation for continuous flow by passing to the limit of a finite change in flow quantities occurring over a very short distance. By integrating the mechanical energy equation across the boundary layer one obtains

$$\frac{\partial}{\partial x}\left[\int_0^\delta \left(\frac{\rho u^3}{2}\right) dy\right] - \left(\frac{\rho u^3}{2}\right)_{y=\delta} \frac{d\delta}{dx} + (\rho v)_\delta \left(\frac{u_\delta^{\,2}}{2}\right)$$

$$= \; - \left(\frac{dp}{dx}\right) \int_0^\delta u\, dy - \int_0^\delta \mu \left(\frac{\partial u}{\partial y}\right)^2 dy \tag{22}$$

In a supercritical-subcritical jump $\frac{d\delta}{dx}$, $\frac{dp}{dx}$ and the rate of change of mechanical energy flux all $\rightarrow \infty$, while the dissipation term and the term $(\rho v)_\delta \left(\frac{u_\delta^{\,2}}{2}\right)$ arising from the streamline inclination remain finite, and are therefore neglected in comparison to the other terms. Then Eq. (22) takes a form quite similar to the integrated momentum equation, except that δ is replaced by $\int_0^\delta u\,dy = K$. When Eq. (22) is multiplied by $\Delta x = \Delta x_1 + \Delta x_2$ and $\Delta x \rightarrow 0$, we find

<u>MECHANICAL ENERGY (MOMENT OF MOMENTUM)</u>

$$G_2 - G_1 \;=\; (\rho_e u_e^{\,3})_1 \; (\delta_2 - \delta_1) - 2K_2 \; (p_2 - p_1) \tag{23}$$

where

$$G \;=\; \int_0^\delta \rho u^3 dy \;=\; \rho_\infty a_\infty u_e^{\,2} M_e \, \delta_i^* (Z-J) \tag{24}$$

and

$$K \;=\; \int_0^\delta u\,dy = \frac{\rho_\infty}{\rho_e} a_\infty M_e \, \delta_i^* \Big[(1+m_e)(Z+S_w T^*) - m_e (Z-J)\Big] \tag{25}$$

Strictly speaking some average value of K should be used in Eq. (23), but we employed K_2 here by analogy with the momentum equation [Eq. (17)], and the difference is very small in any case.

As it turns out, the relative change in Mach number M_e across a laminar supercritical-subcritical jump is small, so the pressure change is connected to the velocity difference by the approximate relation

$$p_2 - p_1 \cong -\tfrac{1}{2}\left[(\rho_e u_e)_1 + (\rho_e u_e)_2\right]\left(u_{e_2} - u_{e_1}\right) \tag{26}$$

By substituting the expressions for $\dot{m}$, I, G, K and δ into Eq. (16)-(18) and Eq. (23), one obtains the relation

$$\frac{M_{e_2}}{M_{e_1}}\,\frac{\delta_{i\,2}^{*}}{\delta_{i\,1}^{*}}\left[m_{e_2}\,B_2 + \left(1 - \frac{\rho_{e_2}\,u_{e_2}}{\rho_{e_2}\,u_{e_1}}\right)Z_2\right] = \frac{\rho_{e_2}}{\rho_{e_1}}\,\frac{u_{e_2}}{u_{e_1}}\,m_{e_1}\,B_1 \tag{27}$$

from the continuity equation [Eq. (16)]; by utilizing this relation in the momentum and mechanical energy equations, these equations become

$$\left[\frac{M_{e_2}}{M_{e_1}}\,\frac{\delta_{i\,2}^{*}}{\delta_{i\,1}^{*}}\,\mathcal{K}_2 - \mathcal{K}_1\right] = \left[1 - \frac{u_{e_2}}{u_{e_1}}\right]\left[\frac{M_{e_2}}{M_{e_1}}\,\frac{\delta_{i\,2}^{*}}{\delta_{i\,1}^{*}}\right]\left[\mathcal{K}_2 - Z_2 + \left(\frac{\rho_{e_1}\,u_{e_1} + \rho_{e_2}\,u_{e_2}}{2\rho_{e_2}\,u_{e_2}}\right)\left(m_{e_2}\,B_2 + Z_2\right)\right] \tag{28}$$

and

$$\left[\frac{M_{e_2}}{M_{e_1}}\,\frac{\delta_{i\,2}^{*}}{\delta_{i\,1}^{*}}\,J_2 - J_1\right] = \left[1 - \frac{u_{e_2}}{u_{e_1}}\right]\left[\frac{M_{e_2}}{M_{e_1}}\,\frac{\delta_{i\,2}^{*}}{\delta_{i\,1}^{*}}\right]\left\{\left(1 + \frac{u_{e_2}}{u_{e_1}}\right)\left(J_2 - Z_2\right) + 2\left(\frac{u_{e_2}}{u_{e_1}}\right)\left(\frac{\rho_{e_1}\,u_{e_2} + \rho_{e_2}\,u_{e_2}}{2\,\rho_{e_2}\,u_{e_2}}\right)\left[(1+m_{e_2})S_w\,T_2^{*} + m_{e_2}\,J_2 + Z_2\right]\right\} \tag{29}$$

Eliminating $\dfrac{\delta_{i\,2}^{*}}{\delta_{i\,1}^{*}}$ from Eq. (27)-(29), one obtains

$$\left[J_2\mathcal{X}_1 - J_1\mathcal{X}_2\right] = \left[1 - \frac{u_{e_2}}{u_{e_1}}\right]\left\{\left[Z_2 - \mathcal{X}_2 - \left(\frac{\rho_{e_1} u_{e_1} + \rho_{e_2} u_{e_2}}{2\,\rho_{e_2} u_{e_2}}\right)\left(m_{e_2} B_2 + Z_2\right)\right] J_1\right.$$

$$\left. - \left[\left(1 + \frac{u_{e_2}}{u_{e_1}}\right)\left(Z_2 - J_2\right) - 2\,\frac{u_{e_2}}{u_{e_1}}\left(\frac{\rho_{e_1} u_{e_1} + \rho_{e_2} u_{e_2}}{2\,\rho_{e_2} u_{e_2}}\right)\left(m_{e_2} J_2 + Z_2\right)\right]\mathcal{X}_1\right\} \qquad (30)$$

and

$$\left[m_{e_2} B_2 \mathcal{X}_1 - m_{e_1} B_1 \mathcal{X}_2\right] = \left[1 - \frac{u_{e_2}}{u_{e_1}}\right]\left[Z_2 - \mathcal{X}_2 - \left(\frac{\rho_{e_1} u_{e_1} + \rho_{e_2} u_{e_2}}{2\,\rho_{e_2} u_{e_2}}\right)\left(m_{e_2} B_2 + Z_2\right)\right] m_{e_1} B_1$$

$$- \left[\frac{\rho_{e_1} u_{e_1}}{\rho_{e_2} u_{e_2}} - 1\right]\left[m_{e_2} B_2 + Z_2\right]\mathcal{X}_1 \qquad (31)$$

These equations furnish two relations between $\mathcal{X}_2$ (or a_2) and M_{e_2}.

The method of solution is described in the Appendix.

In the limiting case of an infinitesimal "jump" the quantity $\left(1 - \frac{u_{e_2}}{u_{e_1}}\right) \rightarrow 0$ and Eq. (28) takes the form

$$\left(M_e\,\delta_i^*\mathcal{X}\right)_2 - \left(M_e\,\delta_i^*\mathcal{X}\right)_1 \rightarrow - \frac{\Delta u_e}{u_e}\,(1+m_{e_2})(\mathcal{X}_2 + 1 - \tilde{e}_2) \qquad (32)$$

while Eq. (29) becomes

$$\left(M_e\,\delta_i^* J\right)_2 - \left(M_e\,\delta_i^* J\right)_1 \cong -2\,\frac{\Delta u_e}{u_e}\,(1+m_{e_2})(S_w T_2^* + J_2) \qquad (33)$$

Now, by rewriting the two basic differential equations for continuous (non-adiabatic) flow [Eq. (2) and (3)], in the form

$$\left[M_e \mathcal{X}\frac{d\delta_i^*}{dx} + M_e\,\delta_i^*\frac{d\mathcal{X}}{dx} + \mathcal{X}\,\delta_i^*\frac{dM_e}{dx}\right] + (\mathcal{X} + 1 - \tilde{e})\frac{dM_e}{dx} = (\text{R.H.S.})M_e \qquad (34)$$

and

$$\left[M_e J\,\frac{d\,\delta_i^*}{dx} + M_e\,\delta_i^*\frac{dJ}{dx} + \delta_i^* J\,\frac{dM_e}{dx}\right] + 2(J + S_w T^*)\frac{dM_e}{dx} = (\text{R.H.S.})M_e \qquad (35)$$

and making use of the relation $\frac{dM_e}{M_e}\frac{1}{1+m_e} = \frac{du_e}{u_e}$, one sees that the last two equations are identical to the two corresponding jump equations in the limit $\Delta x \to 0$ with the R. H. S. $\to 0$. One can show also that the continuity relation [Eq. (16) and (21)] for an infinitesimal "jump" reduces to the continuity equation for continuous flow [Eq. (1)] in the limit $\Delta x \to 0$, with its R. H. S. $\to 0$. In other words the equations for an infinitesimal jump correspond to the equations obtained from Eq. (1)-(3) by multiplying by Δx and passing to the limit $\Delta x \to 0$.

Now the equations for an infinitesimal jump correspond exactly to the homogeneous form of the continuous flow equations, so that non-trivial solutions exist only when the determinant of the matrix vanishes, i. e. when $D = 0$. We conclude that an infinitesimal jump can occur only at the critical point. The analogy to a normal "shock wave" of infinitesimal strength in a nozzle is complete; such a standing shock wave occurs only at the "throat".

By rewriting Eq. (30) slightly one finds that for adiabatic flow

$$\aleph_2\left(\frac{J_1}{\aleph_1} - \frac{J_2}{\aleph_2}\right) \cong -\left(\frac{M_{e_2}}{M_{e_1}} - 1\right)\left[\aleph_2\left(\frac{J_1}{\aleph_1} - \frac{J_2}{\aleph_2}\right) + \left(\frac{J_1}{\aleph_1} - J_2\right)\right] \tag{30a}$$

As one can see from Fig. 2 and 3, in the region of interest $\left(\frac{J_1}{\aleph_1} - \frac{J_2}{\aleph_2}\right) \gtreqless 0$ when $\aleph_1 \gtreqless \aleph_2$. Also it is certain that $\frac{J_1}{\aleph_1} > J_2$ when $\aleph_1 > \aleph_2$. Therefore, Eq. (30a) shows that a compression or a decrease in Mach number M_e across the jump is always accompanied by a decrease in $\aleph$. When $\aleph_1 = \aleph_{cr}$, we obtain relations across an infinitesimal jump analogous to the expression for an ordinary acoustic wave, e.g.,

$$\left(\frac{\mathscr{V}_{cr}-\mathscr{V}_2}{\mathscr{V}_{cr}}\right) = \left(\frac{M_{e_1}-M_{e_2}}{M_{e_1}}\right)\left[\frac{J_{cr}\left(1-\mathscr{V}_{cr}\right)}{\left(\frac{dJ}{d\mathscr{V}}-\frac{J}{\mathscr{V}}\right)_{cr}}\right] \qquad (36)$$

Thus the flow on the downstream side of a small compressional jump is always subcritical.

One other interesting point of resemblance between these jump relations and an ordinary gasdynamic shock wave is the phenomenon of "hypersonic freezing". When $M_{e_1} \rightarrow \infty$ one finds that the Mach number drops out of Eq. (30) and (31), if these equations are regarded as relations for $\left(1 - \frac{u_{e_2}}{u_{e_1}}\right)$ and $\mathscr{V}_2$. In other words $\mathscr{V}_2$ (and J_2, a_2, etc.) is a unique function of $\mathscr{V}_1$ in the hypersonic limit.

The jump equations [Eq. (30) and (31)] were solved on an IBM 7090 computer utilizing the method discussed in the Appendix and the polynomial curve-fits to $\mathscr{V}$, J and Z discussed in Section 2; the results for some typical cases are illustrated in Figure 11. One sees that the reduction in Mach number across these jumps is indeed very small. Even for $M_{e_1} = 6$ and $a_1 = a_{1\,max} = 3.90$ the relative change in M_e is about 3%, and the corresponding static pressure ratio is about 1.24 across the jump. On the other hand the change in the shape parameter "a" is considerable, especially when $M_{e_1} >> 1$, but the minimum a_2 is about 2.0, still far from separation, and indeed above the Blasius flow. For all the jump conditions investigated the boundary layer thickness <u>decreases</u> across the jump, and mass flux is lost to the "outer" inviscid flow. However, the physical displacement thickness increases slightly across the jump, which is entirely consistent with a compression occurring over a downstream distance of one or two boundary layer thicknesses.

As we have already observed, the behavior of these jumps is strikingly similar in many respects to the ordinary gasdynamic shock wave. For example, the more strongly supercritical is the state upstream of the jump, the more subcritical is the state behind the jump. Also, conditions downstream of the jump become virtually independent of M_{e_1} for $M_{e_1} > 6$ (Fig. 11).

Since the flow downstream of the jump is always subcritical, but far from separation, this flow must generate a self-induced pressure rise along the body surface which produces separation and the beginning of the mixing region in the near wake (Section 4).

IV. FLOW FIELD DOWNSTREAM OF THE JUMP, THROUGH SEPARATION AND INTO THE CONSTANT PRESSURE MIXING REGION

Between the critical point on the cylinder at $\frac{x}{r} = 1.69$ and the pressure minimum at $\frac{x}{r} = 2.18$ we know all the quantities δ_i^*, a, M_e [Fig. (9)], so we can compute a possible jump to subcritical conditions at each location $\frac{x}{r}$. Also the streamline inclination Θ_1 just upstream of the jump is obtained from Eq. (15), and Θ_2 is calculated from Θ_1 by adding the turning angle across the weak compression. Thus at each location $(x/r)_2 = (x/r)_1$ we know all the "initial" conditions $\delta_{i_2}^*$, a_2, M_{e_2} and Θ_2 required to start the computation of the interaction between the now subcritical viscous flow and the outer flow. These subcritical trajectories are calculated by integrating the full equations [Eq. (1)-(3)], making use of the Prandtl-Meyer relation including the effect of surface curvature [Eq. (5)]. Downstream of the separation point (a = 0) we utilize the curve-fits to $\mathscr{K}$, J, P, R, Z shown in Fig. 2-6 in the region marked "separated flow", where $a(x) = (Y/\delta_i^*)_{U=0}$.

In Fig. 12 we show a subcritical trajectory to separation and beyond for the eigen-solution found in Section VI. Downstream of separation the positive pressure gradient decreases rapidly, partly because the body surface is "falling away" from the tangent to the local streamline at the outer edge of the boundary layer. If the location of the beginning of the "pressure plateau" is identified by $(x/r)_{p.p.}$, then the angular turn measured around the cylinder surface from the jump location to $(x/r)_{p.p.}$ is about 13° in a typical case ($Re_{o,d} = 4 \times 10^4$), and the angular turn from separation to $(x/r)_{p.p.}$ is about 7°.

Downstream of $(x/r)_{p.p.}$ we enter the constant pressure mixing region treated by Reeves and Lees[3]. In this region the basic equations are considerably simplified by dropping the term containing $\frac{dM_e}{dx}$ and ignoring the continuity equation [Eq. (1)]. These reduced equations were solved for $\frac{d(\delta_i^*/r)}{da}$ and $\frac{d(x/r)}{da}$ and integrated up to a value of $a = 0.7$, corresponding to $u^*_{mixing} = 0.56$.

V. NEAR WAKE INTERACTION REGION AND JOINING CONDITIONS

Since the location of the separation point on the body and the length of the constant pressure mixing region are unknown á priori, it is more convenient to begin the calculation of the near-wake interaction solution at the rear stagnation point, where $a = 0$. Starting at this point with a given value of $\left(\frac{\delta_i^*}{r}\right)_{r.s.p.}$ and a given value of $Re_{\infty, d}$, Reeves and Lees[3] have shown that there is only one value of M_e at the rear stagnation point that allows the solution to go through the downstream critical point or "throat" in the wake. The procedure adopted was to integrate the basic equations [Eq. (1)-(3)] downstream of the rear stagnation point with various trial values of $\left(M_e\right)_{r.s.p.}$ until one solution is obtained that passes as close to the singularity at $D = 0$ as possible. Here $P = 0$ in Eq. (2), and the curvature term $\alpha(x)$ in the Prandtl-Meyer relation [Eq. (5)] is absent. It is more convenient to take the reference point "far" downstream, so $Ⓗ = \nu(M_\infty) - \nu(M_e)$. The curve-fits to the functions $\mathcal{K}$, R, J, Z for wake flows given in Ref. 3 were utilized in the integration. In order to fix the downstream conditions we selected $M_{freestream} = 6.0$, or $(M_\infty)_{wake} = 2.5$.

Once the correct value of $(M_e)_{r.s.p.}$ is determined for a given choice of $\left({\delta_i^*}/{r}\right)_{r.s.p.}$ and $Re_{\infty, d}$, Eq. (1)-(3) are integrated in the <u>upstream</u> direction away from the r.s.p. in order to generate a family of possible wake solutions.

At some point in the near-wake region the constant-pressure mixing solution must be joined to the wake interaction solution. For a given value of $Re_{o,d}$ and $M_{freestream}$ the boundary layer growth on the cylinder up to the jump location is determined, but the jump can be placed at any point on the body downstream of the critical point $\left(x/r = 1.69\right)$. For a given jump location the flow is determined completely up to the beginning of the "pressure plateau", but the length of the constant pressure mixing region is arbitrary; any point on the mixing solution curve corresponding to a certain u* is a possible joining point to the wake interaction solution. For a given value of $\left(\delta_i^*/r\right)_{r.s.p.}$ the length of the wake interaction upstream of the rear stagnation point is also arbitrary. Thus, four conditions are required at the matching point in order to determine the complete solution uniquely.

Three conditions are more or less obvious: continuity of M_e, of u*, and of the mass flow above the dividing streamline, which is proportional to $M_e \delta_i^* Z$ [Eq. (19)]. The fourth condition is a geometric constraint; the length of the constant pressure mixing zone and the wake thickness h/r at the joining point must be so determined that the angle Ⓗ of the dividing streamline is compatible with the Prandtl-Meyer turning angle for $(M_e)_{p.p.}$, i.e. (Fig. 1),

$$\frac{\left(d_1/r - h/r\right)}{\left(x/r\right)_{mixing}} = \nu(M_\infty) - \nu(M_e)_{p.p.} \tag{37}$$

where

$$d_1/r = \left(1 + \frac{\delta_{p.p.}}{r}\right) \sin\left[\pi - \left(x/r\right)_{p.p.}\right] \tag{38}$$

These four joining conditions uniquely determine the complete solution for a given pair of values of $Re_{\infty,d}$ and M_∞.

VI. TYPICAL SOLUTION FOR SEPARATION AND NEAR WAKE INTERACTION REGIONS: ADIABATIC CIRCULAR CYLINDER AT $M_o = 6$

In order to illustrate the method of solution described in Sections III-V, a typical case is worked out for the adiabatic circular cylinder at $M_\infty = 2.5$ and $Re_{\infty,d} = 8000$, corresponding to freestream values of $M_o = 6$ and $Re_{o,d} = 4\times10^4$. A useful diagram employed in matching the wake interaction and constant-pressure mixing regions is shown in Figure 13. For every choice of $\left(\frac{\delta_i^*}{r}\right)_{r.s.p.}$ the wake interaction eigensolution is integrated in the upstream direction away from the r.s.p. to produce a locus of pairs of values of M_e and U^*; these curves are labelled "wake solution" in Figure 13. Every point on each of these curves also corresponds to known local values of δ_i^*/r and Z.

Now, for a given trial jump location on the body surface the separating flow is determined up to the pressure plateau, so $M_e = (M_e)_{p.p.}$ is known in the constant-pressure mixing region. The horizontal dashed lines in Figure 13 represent the constant pressure mixing solutions for U^* as a function of δ_i^*/r, for a given jump location. At the intersection of these dashed lines and the full curves calculated from the wake interaction solution M_e and U^* are automatically matched. The correct choice of the remaining two unknowns $(x/r)_{jump}$ and $\left(\frac{\delta_i^*}{r}\right)_{r.s.p.}$ is determined by matching mass flow above the dividing streamline, and satisfying the geometric constraint embodied in Eq. (37) and (38).

Figure 14 shows a comparison between the predicted static pressure distribution on the circular cylinder at $Re_{o,d} = 4\times10^4$ and

Mc Carthy's [2], [11] experimental measurements at two nearby Reynolds numbers of 3.2×10^4 and 4.7×10^4. Evidently the computed base pressure [p(180°)] is somewhat low, but the location of separation on the cylinder is predicted quite accurately. Of course in practice the jump is smeared out over a distance of one or two boundary layer thicknesses.

The constant pressure and near wake interaction regions from the pressure plateau to a point near the neck are shown in Figure 15. As observed by Reeves and Lees[3] the predicted rear stagnation point is located somewhat aft of Dewey's[11] measured location. Presumably the accuracy of the wake interaction solution can be improved, especially at low Reynolds numbers, by utilizing the two-parameter velocity profiles of Reference 12, rather than the one-parameter profiles employed here.

This illustrative example shows that the theoretical approach employing an integral or moment method is fully capable of predicting the location of separation and the entire near wake interaction region for laminar flow, without the introduction of additional ad hoc assumptions or floating parameters. It would be interesting to extend the calculations to show the effect of free stream Reynolds number and/or a cool surface on the location of separation. This general method is applicable not only to blunt bodies, but also to slender bodies with smooth bases, provided only that the radius of curvature at the base is large compared to the boundary layer thickness.

REFERENCES

1. Dewey, C. F., Jr.: "Measurements in Highly Dissipative Regions of Hypersonic Flows. Part II. The Near Wake of a Blunt Body at Hypersonic Speeds," Ph.D. Thesis, California Institute of Technology (1963), also AIAA J. 3, 1001-1010 (1965).

2. McCarthy, J. F., Jr. and Kubota, T.: "A Study of Wakes Behind a Circular Cylinder at M = 5.7," AIAA J. 2, 629-636 (1964).

3. Reeves, B. L. and Lees, L.: "Theory of the Laminar Near Wake of Blunt Bodies in Hypersonic Flow," AIAA J., 3, 2061-2074 (1965).

4. Chapman, D. R., Kuehn, D. M., and Larson, H. K.: "Investigation of Separated Flows in Supersonic and Subsonic Streams with Emphasis on the Effect of Transition," NACA Rept. 1356 (1958).

5. Lees, L. and Reeves, B. L.: "Supersonic Separated and Reattaching Laminar Flows: I. General Theory and Application to Adiabatic Boundary Layer-Shock Wave Interactions," AIAA J. 2, 1907-1920 (1964).

6. Crocco, L. and Lees, L.: "A Mixing Theory for the Interaction Between Dissipative Flows and Nearly Isentropic Streams," J. Aerospace Sci. 19, 649-676 (1952).

7. Crocco, L.: "Considerations on the Shock-Boundary Layer Interaction," Proceedings of the Conference on High-Speed Aeronautics, Polytechnic Institute of Brooklyn, pp. 75-112 (January 20-22, 1955).

8. Crocco, L. and Probstein, R. F.: "The Peak Pressure Rise Across an Oblique Shock Emerging from a Turbulent Boundary Layer Over a Plane Surface," Princeton Univ. Aero. Eng. Dept., Rept. 254 (March 1954).

9. Stewartson, K.: "Further Solutions of the Falkner-Skan Equation," Proc. Cambridge Phil. Soc. 50, 454-465 (1954).

10. Cohen, C. B. and Reshotko, E.: "Similar Solutions for the Compressible Laminar Boundary Layer with Heat Transfer and Pressure Gradient," NACA Rept. 1293 (1956).

REFERENCES (Cont'd)

11. McCarthy, J. F. Jr.: "Hypersonic Wakes," GALCIT Hypersonic Research Project, Memorandum No. 67 (1962).

12. Webb, W. H., R. J. Golik, F. W. Vogenitz and L. Lees: "A Multimoment Integral Theory for the Laminar Supersonic Near Wake," Proceedings of the 1965 Heat Transfer and Fluid Mechanics Institute, Stanford University Press, Stanford, California, pp. 168-189. See also "Further Results of Viscous Interaction Theory for the Laminar Supersonic Near Wake," TRW Systems Report No. 4456-6008-R0000, March, 1966 (Redondo Beach, Calif.)

APPENDIX A

SOLUTION OF THE JUMP EQUATIONS

The two algebraic relations for $\mathcal{V}_2$ (or a_2) and M_{e_2} are given by Eq. (30) and (31), Section III. Since these equations involve the differences between quantities which are nearly equal, it is useful to expand the downstream quantities, $\mathcal{V}_2$ and M_{e_2}, in terms of their upstream values. Defining the quantities η and μ as follows;

$$\eta = \mathcal{V}_1 - \mathcal{V}_2 \tag{A1}$$

$$\mu = \frac{M_{e_1}}{M_{e_2}} - 1 \tag{A2}$$

one can expand the jump equations, Eq. (30) and (31), in powers of these quantities, where, for example

$$1 - \frac{u_{e_2}}{u_{e_1}} = \left(\frac{1}{1+m_{e_1}}\right)\mu + \frac{1}{1+m_{e_1}}\left[1 - \frac{3\, m_{e_1}}{2(1+m_{e_1})}\right]\mu^2 + \text{---}$$

and

$$J_1 - J_2 = \left(\frac{dJ}{d\mathcal{V}}\right)_1 \eta - \left(\frac{d^2J}{d\mathcal{V}^2}\right)_1 \frac{\eta^2}{2} + \text{---}$$

Retaining terms to second order, Eq. (30) and (31) can be expressed in the form

$$A_1\eta + A_2\eta^2 + A_3\eta\mu + A_4\,\mu + A_5\,\mu^2 = 0 \tag{A3}$$

$$B_1\eta + B_2\eta^2 + B_3\eta\mu + B_4\,\mu + B_5\,\mu^2 = 0 \tag{A4}$$

where, for adiabatic flow,

$$A_1 = J - \mathcal{V}\frac{dJ}{d\mathcal{V}} \tag{A5}$$

$$A_2 = \frac{1}{2}\mathcal{V}\frac{d^2J}{d\mathcal{V}^2}$$

$$A_3 = 2\mathcal{V}\frac{dJ}{d\mathcal{V}} - J$$

$$A_4 = (1-\mathcal{V})\,J$$

$$A_5 = \mathcal{V}\left[2m_e J + J + Z\right]\left[\frac{1}{(1+m_e)^2}\right] - J(1-\mathcal{V})\left[1 + \frac{m_e}{2(1+m_e)}\right]$$
$$+ \frac{1}{2}\left[(2\mathcal{V}-J)Z - (1+m_e-m_e\mathcal{V})\,J\right]\left[\frac{M_e^2-1}{(1+m_e)^2}\right]$$

and

$$B_1 = 1 + m_e \tag{A6}$$

$$B_2 = 0$$

$$B_3 = \left[1+m_e+m_e\mathcal{V}+\mathcal{V}\frac{dZ}{d\mathcal{V}}\right]\left[\frac{M_e^2-1}{1+m_e}\right] - \left[1+m_e-m_e\mathcal{V}\right]$$

$$B_4 = (1+\mathcal{V})[1+m_e-m_e\mathcal{V}] - \mathcal{V}[1+m_e+m_e\mathcal{V}+Z]\left[\frac{M_e^2-1}{1+m_e}\right]$$

$$B_5 = (1+\mathcal{V})\left[3m_e\mathcal{V} - (1+m_e+m_e\mathcal{V})\left(1 + \frac{m_e}{2(1+m_e)}\right)\right]$$
$$- \mathcal{V}[1+m_e+m_e\mathcal{V}+Z]\left[1 - \frac{3m_e}{2(1+m_e)} + M_e^2\left(\frac{2\gamma-1}{\gamma-1}\frac{m_e}{1+m_e} - \frac{5}{2}\right)\right]\left[\frac{1}{1+m_e}\right]$$
$$+ \frac{1}{2}[1+m_e+m_e\mathcal{V}]\,[(1+m_e)(1+\mathcal{V}) - (Z-\mathcal{V})]\left[\frac{M_e^2-1}{(1+m_e)^2}\right]$$

where all quantities are evaluated at the upstream station and hence are known. The solution of the two algebraic relations, Eq. (A3) and (A4), using the definitions given above, is now straightforward. Some typical jumps are shown in Figure 11.

TABLE 1-A

$S_w = 0$		SEPARATED PROFILES							
Sym	#	C_0	C_1	C_2	C_3	C_4	C_5	C_6	C_7
$\mathcal{V}$	1	.24711	-.25057	-.43012	.14296	-.42670	-10.85874	38.74254	-31.20919
	2	.28529	-.88415	.66680	.25024	-.32298	---	---	---
J	1	.37372	-.42859	.33036	-5.15165	10.59644	-5.81736	---	---
	2	.27561	-.12875	-1.03947	.37254	1.98688	-1.52324	---	---
Z	1	1.03539	-1.02605	-1.12405	-1.14556	3.34341	---	---	---
	2	1.06176	-2.03101	.99390	---	---	---	---	---
R	3	1.25782	1.09008	7.01736	-33.87617	196.76883	-371.97621	244.30946	---
P	1	---	-1.19450	-.70990	-7.12530	20.85679	-100.27285	310.23943	-263.58721
	2	-3.35578	6.96684	-3.70573	---	---	---	---	---
$\frac{d\mathcal{V}}{da}$	4	-.25057	-.86024	.42888	-1.70682	-54.29370	232.45525	-218.46436	---
	5	-3.61900	9.34395	-1.02866	-13.19952	8.68729	---	---	---
$dJ/d\mathcal{V}$	1	1.50031	-.84045	3.32376	-13.86684	5.47666	30.17701	---	---
$1/dJ/d\mathcal{V}$	2	6.08644	-15.13135	9.54471	---	---	---	---	---

NOTE: 1. $0 \le a \le 0.6$
2. $0.6 \le a \le 0.8$
3. $0 \le a \le 0.8$
4. $0 \le a \le 0.56$
5. $0.56 \le a \le 0.8$

TABLE 1-B

$S_w = 0$		ATTACHED PROFILES					
Sym	#	C_0	C_1	C_2	C_3	C_4	C_5
$\mathcal{H}$	6	.24711	.110560	-.021223	.0043455	-.00097238	.00009921
J	6	.37372	.167689	-.023356	.0057239	-.00174700	.00019124
Z	6	1.03539	.483731	-.015025	.0260954	-.00369675	----
R	6	1.25782	-.555497	.319639	-.0907667	-.01398307	-.00093482
P	6	----	.487447	-.099274	.0096044	-.00031106	----
$d\mathcal{H}/da$	6	.11056	-.042447	.013036	-.0038895	.00049603	----
$dJ/d\mathcal{H}$	6	1.50031	.281050	-.042867	.0026238	----	----

NOTE: 6. $0 \le a \le 3.9$

TABLE 2-A

$S_w = -0.8$		SEPARATED PROFILES						
Sym	#	C_0	C_1	C_2	C_3	C_4	C_5	C_6
$\mathcal{V}$	1	.21360	-.06348	-1.82056	10.55762	-37.08205	57.61391	-31.35775
	2	.78866	-3.04566	3.93969	-1.70572	----	----	----
J	1	.31943	-.19173	-.86790	3.43592	-15.76816	28.64974	-16.52933
	2	.74968	-2.04855	1.03298	1.45265	-1.22712	----	----
Z	3	.85886	-.55378	-.28422	-6.23556	12.58922	-6.47769	----
E	1	.51990	-.03461	-1.17385	9.95019	-40.19250	76.74178	-52.87887
	2	.44424	-2.24455	5.83444	4.44263	-17.39677	9.89966	----
R	3	1.46008	-.39010	28.23864	-174.51371	579.14401	-831.39551	449.01662
P	1	----	-.67296	1.87130	-18.26659	32.78362	-13.05966	----
	2	.29212	-4.39870	4.26208	4.77737	-5.10503	----	----
Q	1	.82606	-.04372	2.56044	-25.88076	111.73742	-239.12252	174.28324
	2	5.42072	-10.54094	-12.75293	39.05220	-21.53288	----	----
$d\mathcal{V}/da$	1	-.14158	-.73754	-.63091	6.22963	-66.14745	190.67465	-148.91834
	2	-4.79632	13.56027	-7.07824	-8.66383	7.10104	----	----
$dJ/d\mathcal{V}$	1	1.47875	-1.08822	6.76658	-27.62517	34.34173	----	----
$1/dJ/d\mathcal{V}$	2	-5.04616	25.17297	-24.65823	-15.64807	21.39078	----	----
$dE/d\mathcal{V}$	1	.50746	.15517	-15.60179	54.93670	-74.33704	-35.40025	----
$1/dE/d\mathcal{V}$	2	-6.26050	23.56503	-30.39277	13.34383	----	----	----

NOTE: 1. $0 \le a \le 0.6$
2. $0.6 \le a \le 0.8$
3. $0 \le a \le 0.8$

TABLE 2-B

$S_w = -0.8$				ATTACHED PROFILES				
Sym	#	C_0	C_1	C_2	C_3	C_4	C_5	C_6
$\mathcal{X}$	6	.21360	.145588	-.025565	-.0018629	.00153453	-.00016560	----
J	6	.31943	.218145	-.025303	-.0023565	.00069938	----	----
Z	6	.85886	.575135	-.070016	.1186249	-.04380291	.00470067	----
E	6	.51990	.105266	-.028593	.0766663	-.01944677	-.00175991	.000659786
R	6	1.46008	-.979128	.664125	-.2272662	.04041507	-.00292428	----
P	6	----	.533067	-.134181	.0078590	.00442000	-.00065180	----
Q	6	.82606	-.064380	-.092813	.0138677	.00745762	-.00149547	----
$d\mathcal{X}/da$	6	.14559	-.051131	-.005589	.0061381	-.00082798	----	----
$dJ/d\mathcal{X}$	6	1.47875	.304088	-.042964	----	----	----	----
$dE/d\mathcal{X}$	7	.50746	1.191231	-.036567	-.2312475	.91079601	-.32829779	----
	8	-25.82618	41.284020	-20.124680	4.2571941	-.34292145	----	----

NOTE: 6. $0 \le a \le 3.9$
7. $0 \le a \le 1.7$
8. $1.6 \le a \le 3.9$

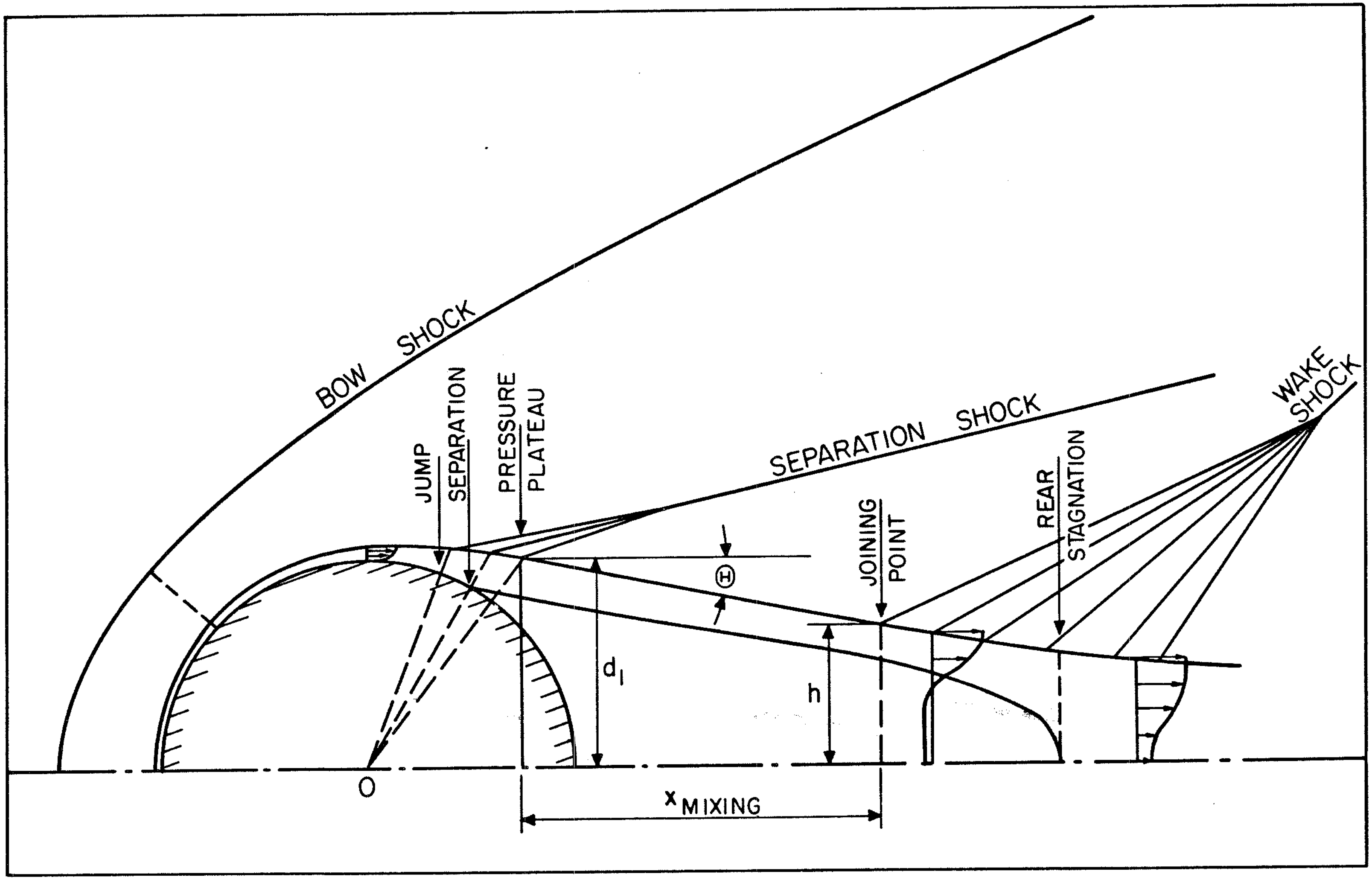

FIG. 1. SEPARATION AND NEAR-WAKE INTERACTION REGIONS FOR A BLUNT BODY AT HYPERSONIC SPEEDS (SCHEMATIC)

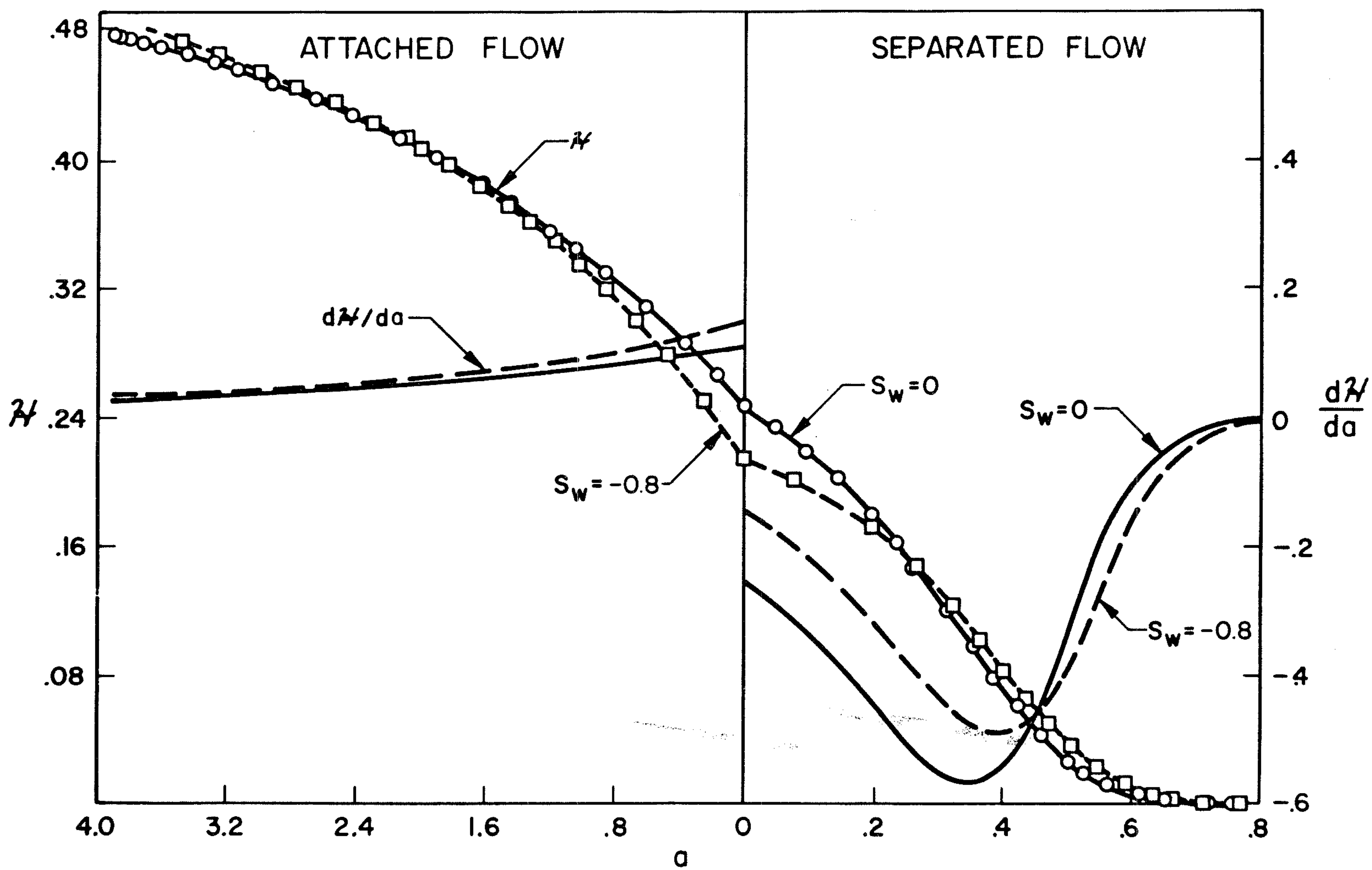

FIG. 2. THEORETICAL $\mathcal{H}$ AND $\frac{d\mathcal{H}}{da}$ DISTRIBUTIONS FOR FLOWS NEAR A SOLID SURFACE

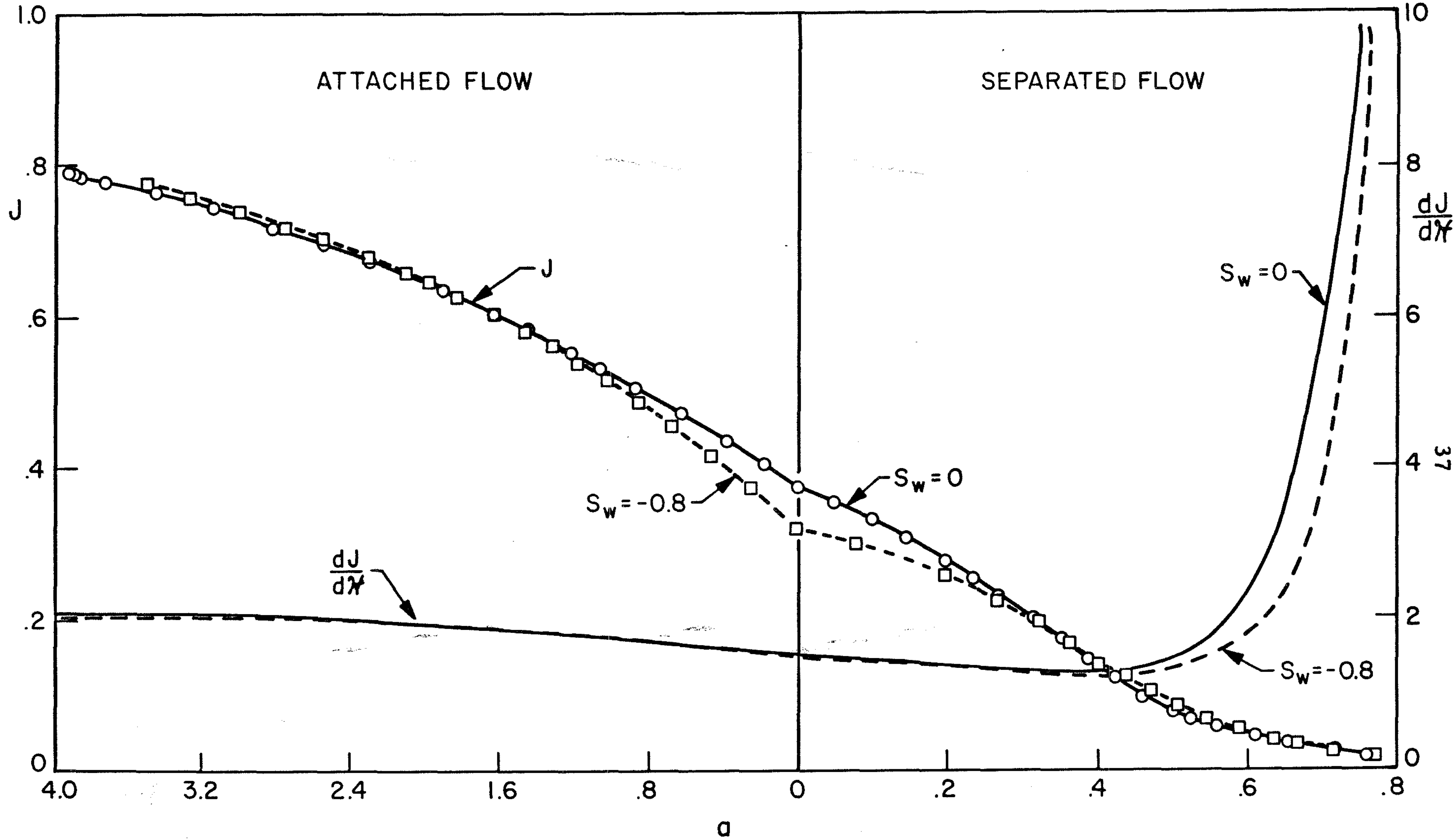

FIG. 3. THEORETICAL J AND $\frac{dJ}{d\chi}$ DISTRIBUTIONS FOR FLOWS NEAR A SOLID SURFACE

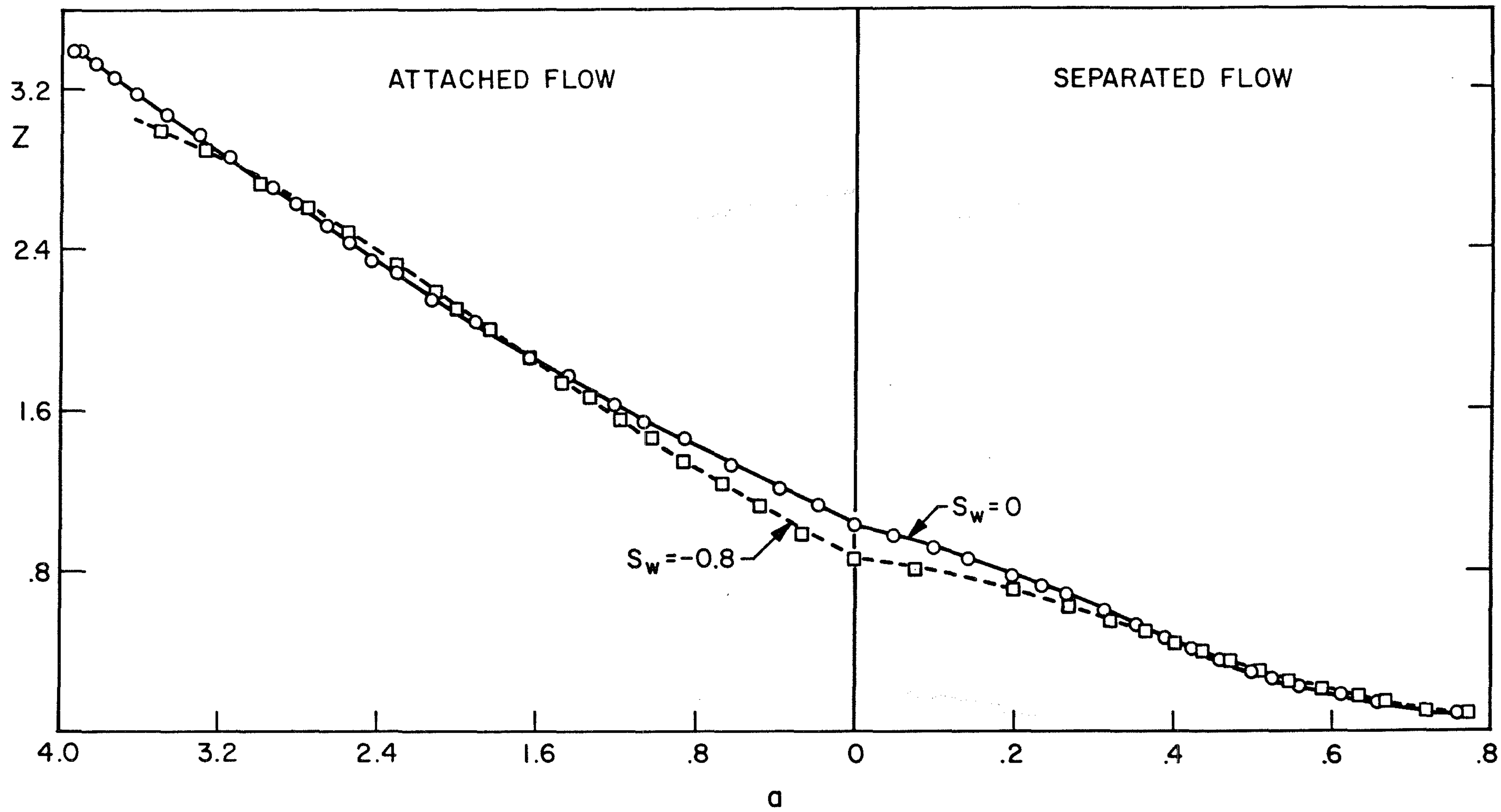

FIG. 4 THEORETICAL Z DISTRIBUTION FOR FLOWS NEAR A SOLID SURFACE

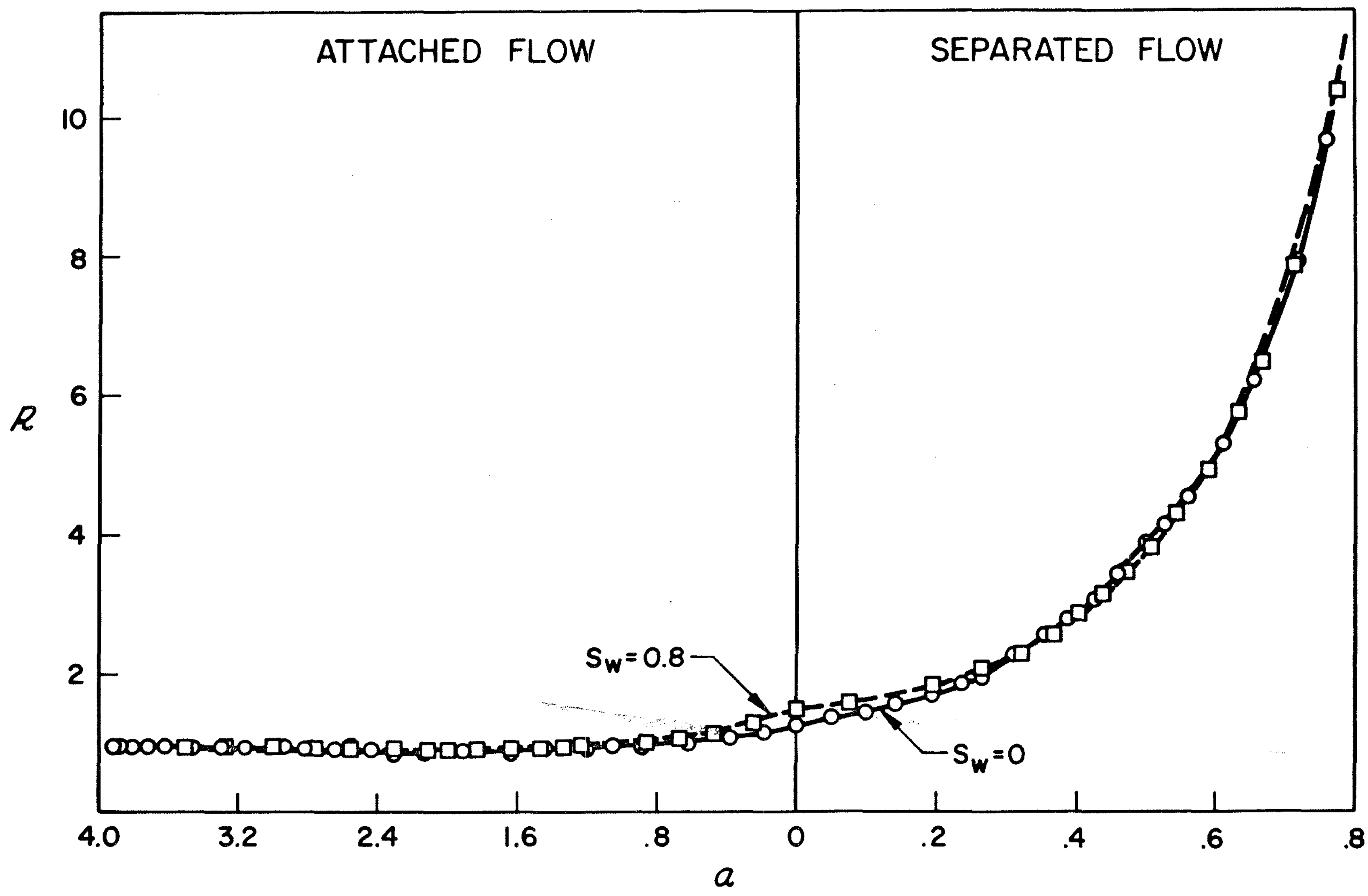

FIG. 5. THEORETICAL R DISTRIBUTION FOR FLOWS NEAR A SOLID SURFACE

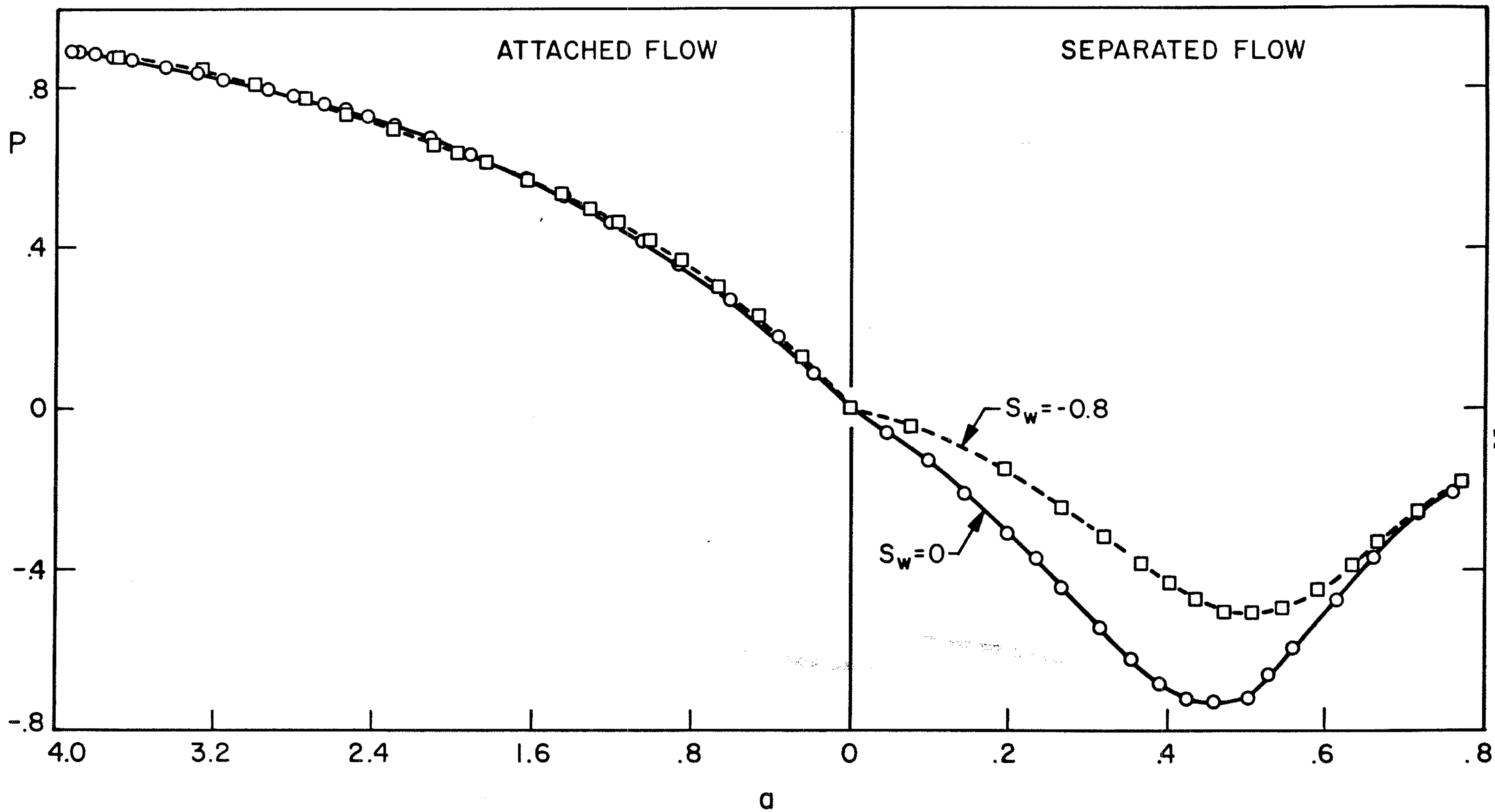

FIG. 6. THEORETICAL P DISTRIBUTION FOR FLOWS NEAR A SOLID SURFACE

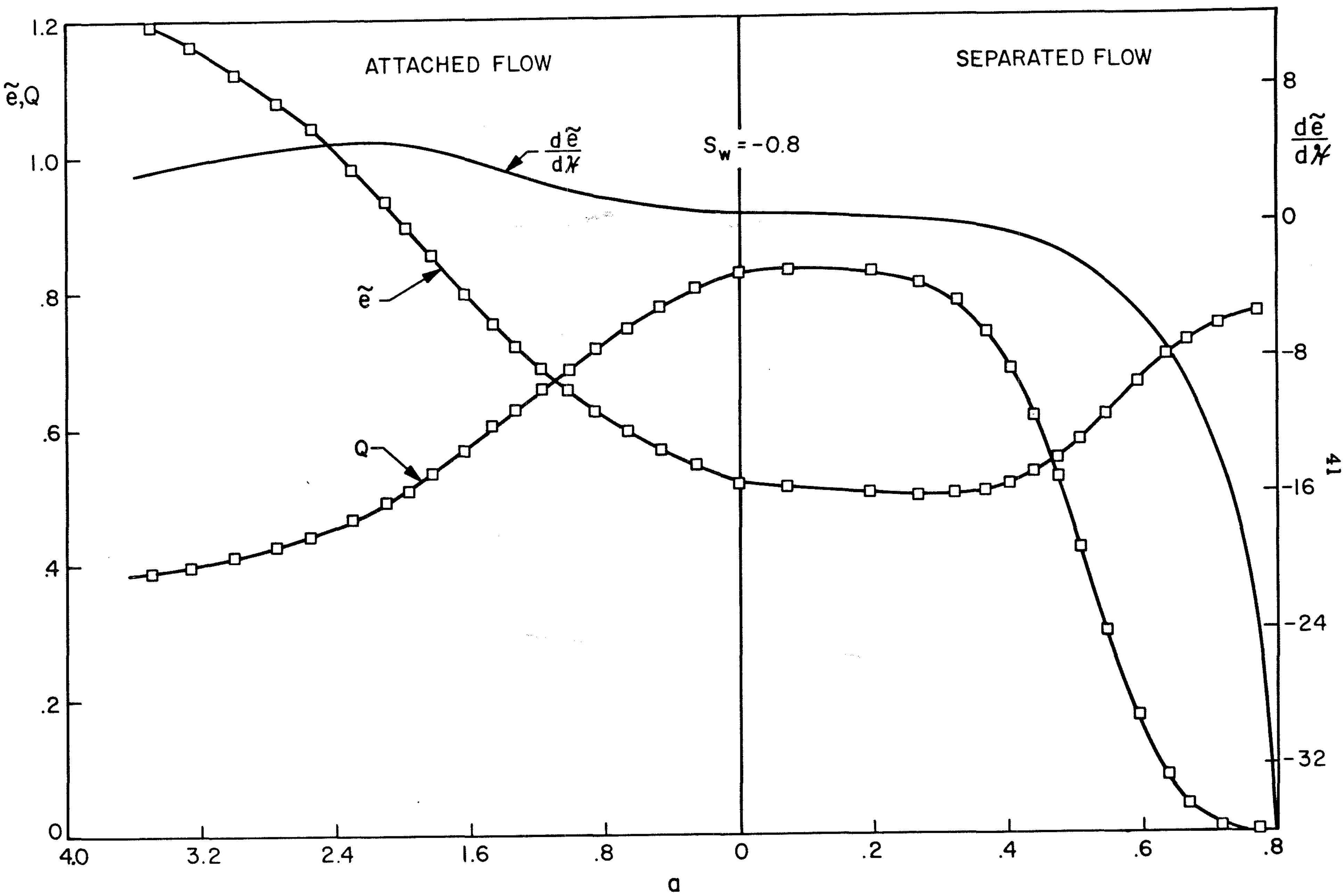

FIG. 7. THEORETICAL $\tilde{e}$ AND Q DISTRIBUTIONS FOR FLOWS NEAR A SOLID SURFACE.

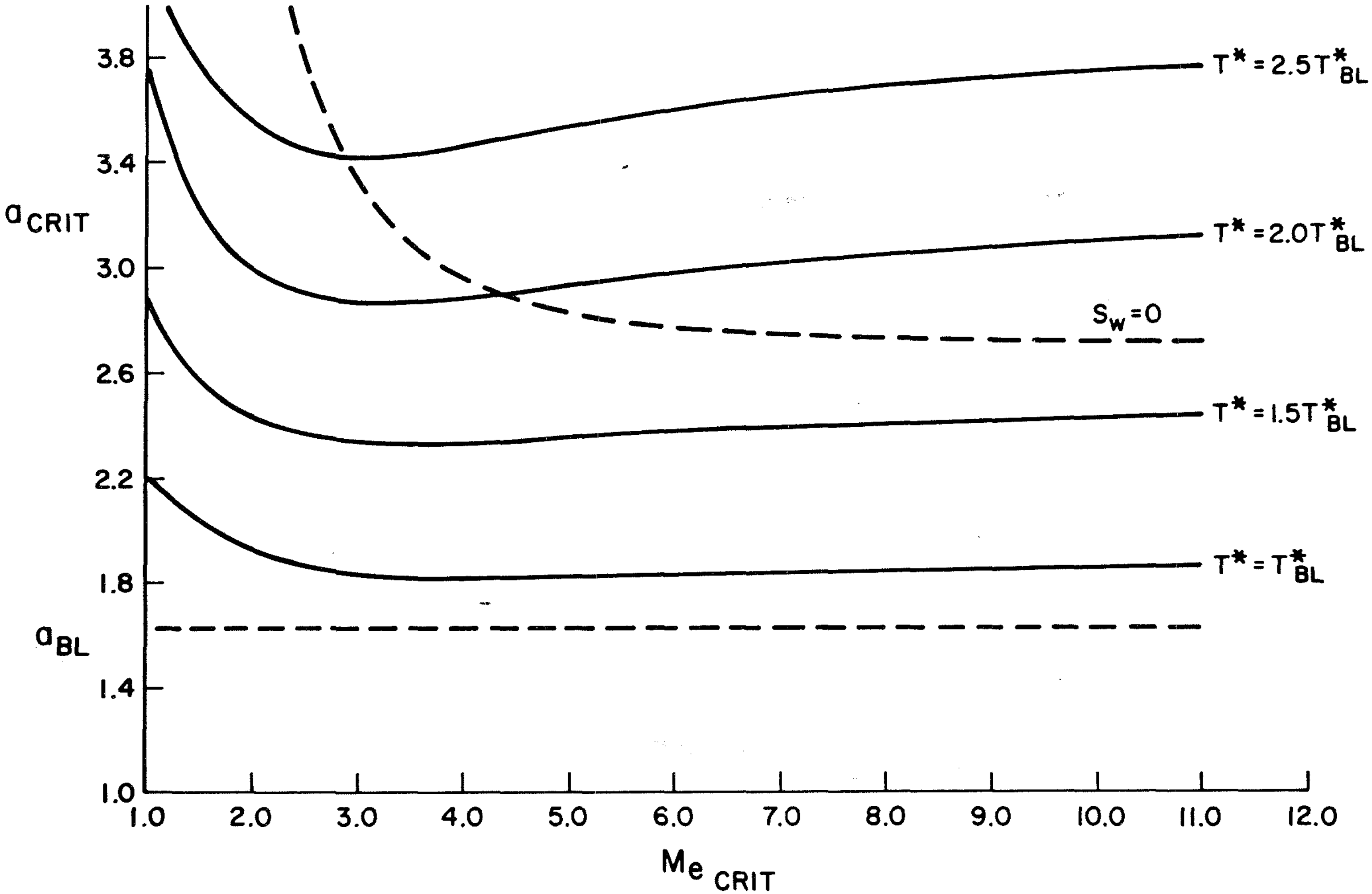

FIG. 8. LOCUS OF CRITICAL POINTS

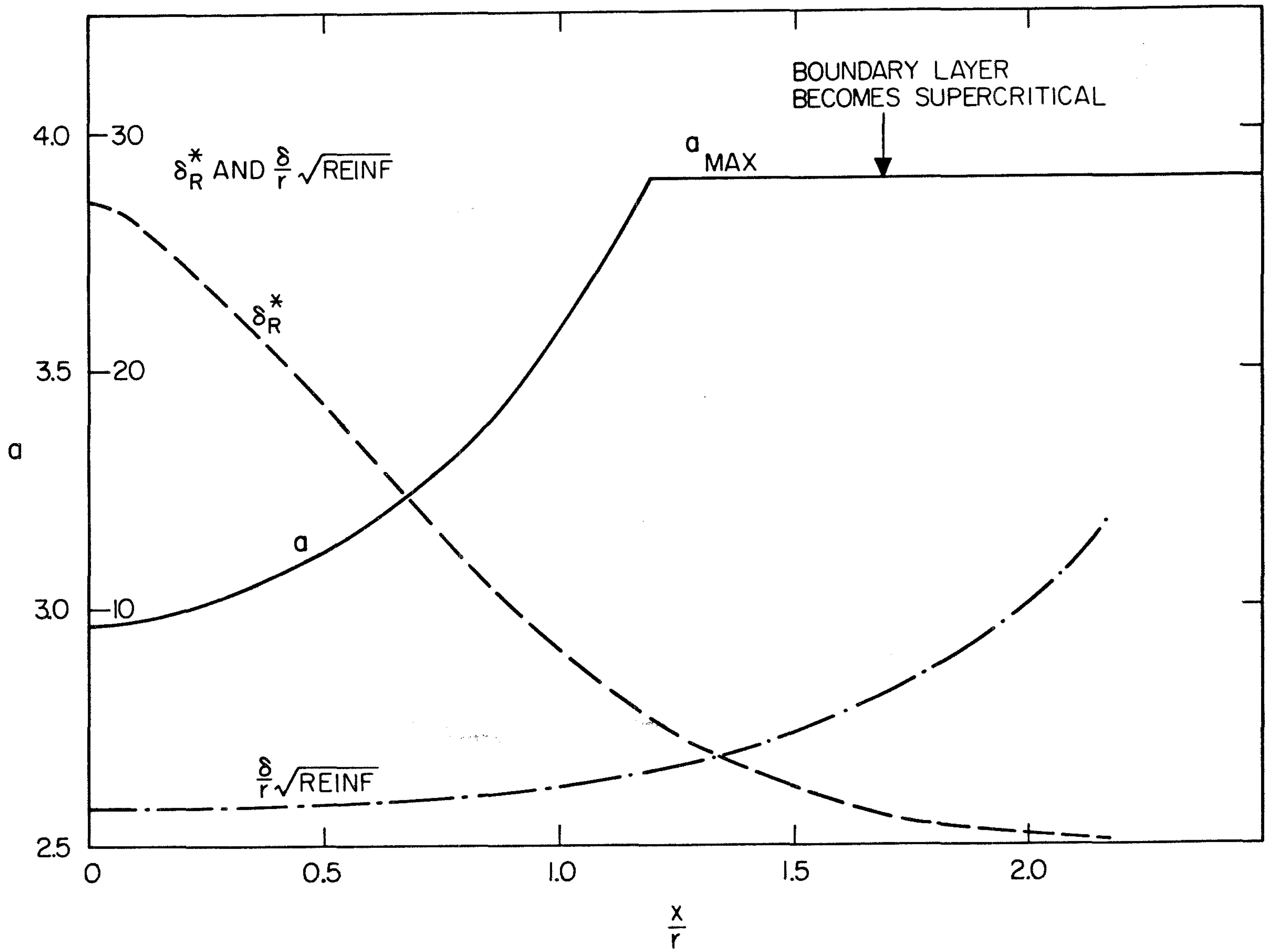

FIG. 9. DISTRIBUTION OF δ_r*, $\frac{\delta}{r}$ AND "a" OVER ADIABATIC CYLINDER

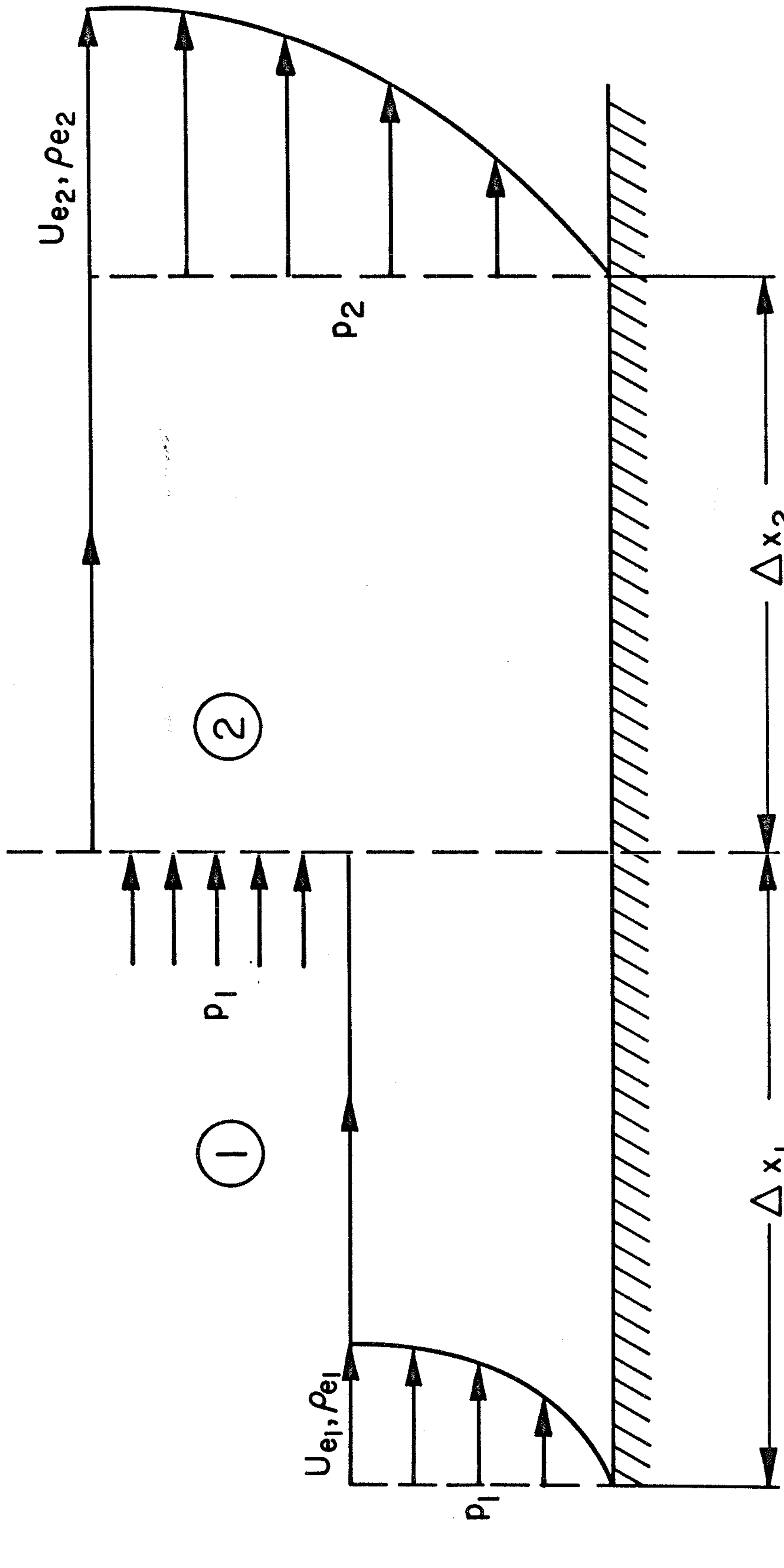

FIG. 10 MODEL FOR SUPERCRITICAL - SUBCRITICAL JUMP

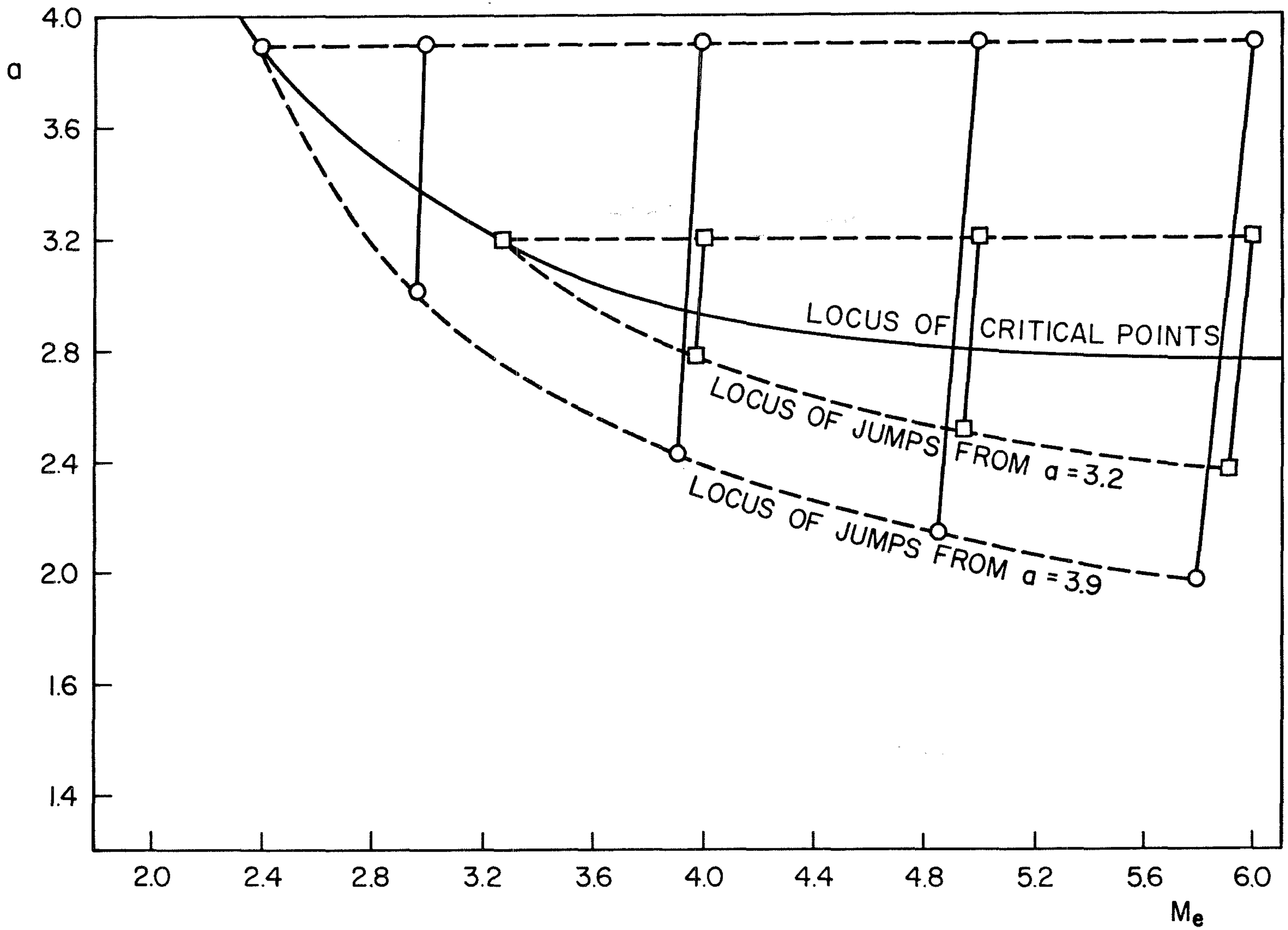

FIG. 11. TYPICAL LAMINAR SUPERCRITICAL - SUBCRITICAL JUMPS

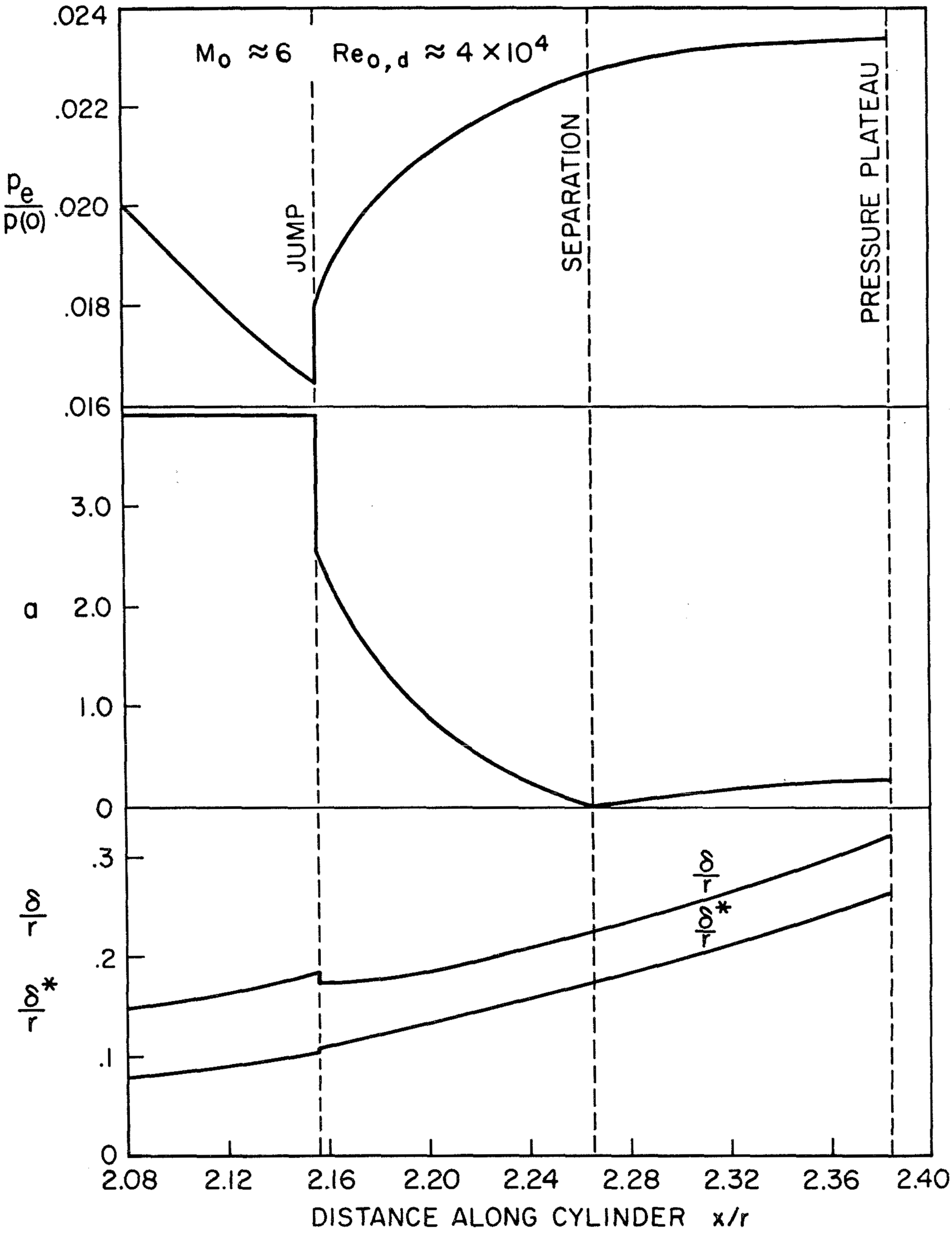

FIG. 12. INTERACTION IN VICINITY OF JUMP

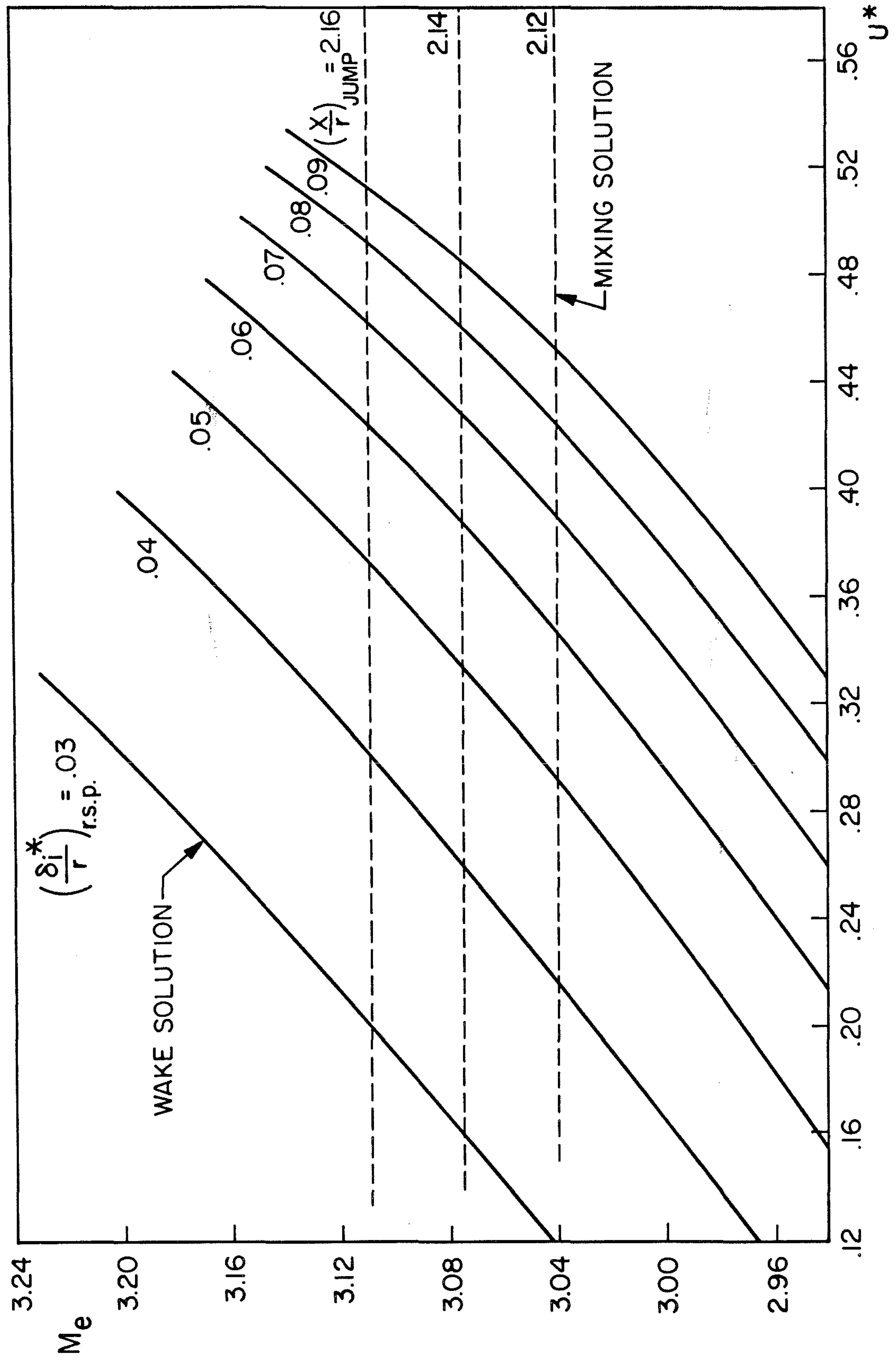

FIG. 13. MATCHING OF MIXING AND WAKE SOLUTIONS

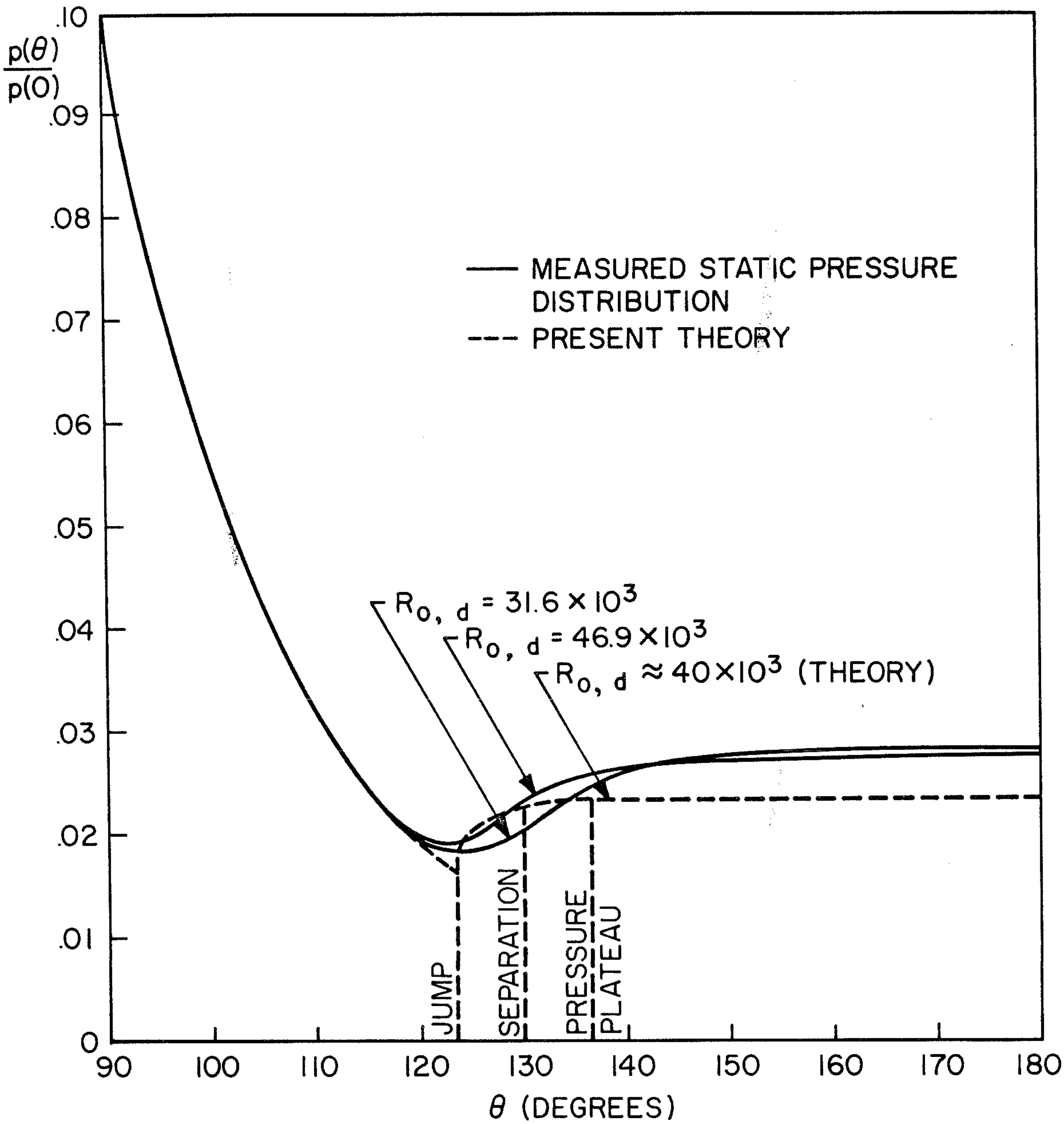

FIG. 14. COMPARISON OF THEORY WITH Mc CARTHY'S EXPERIMENTS

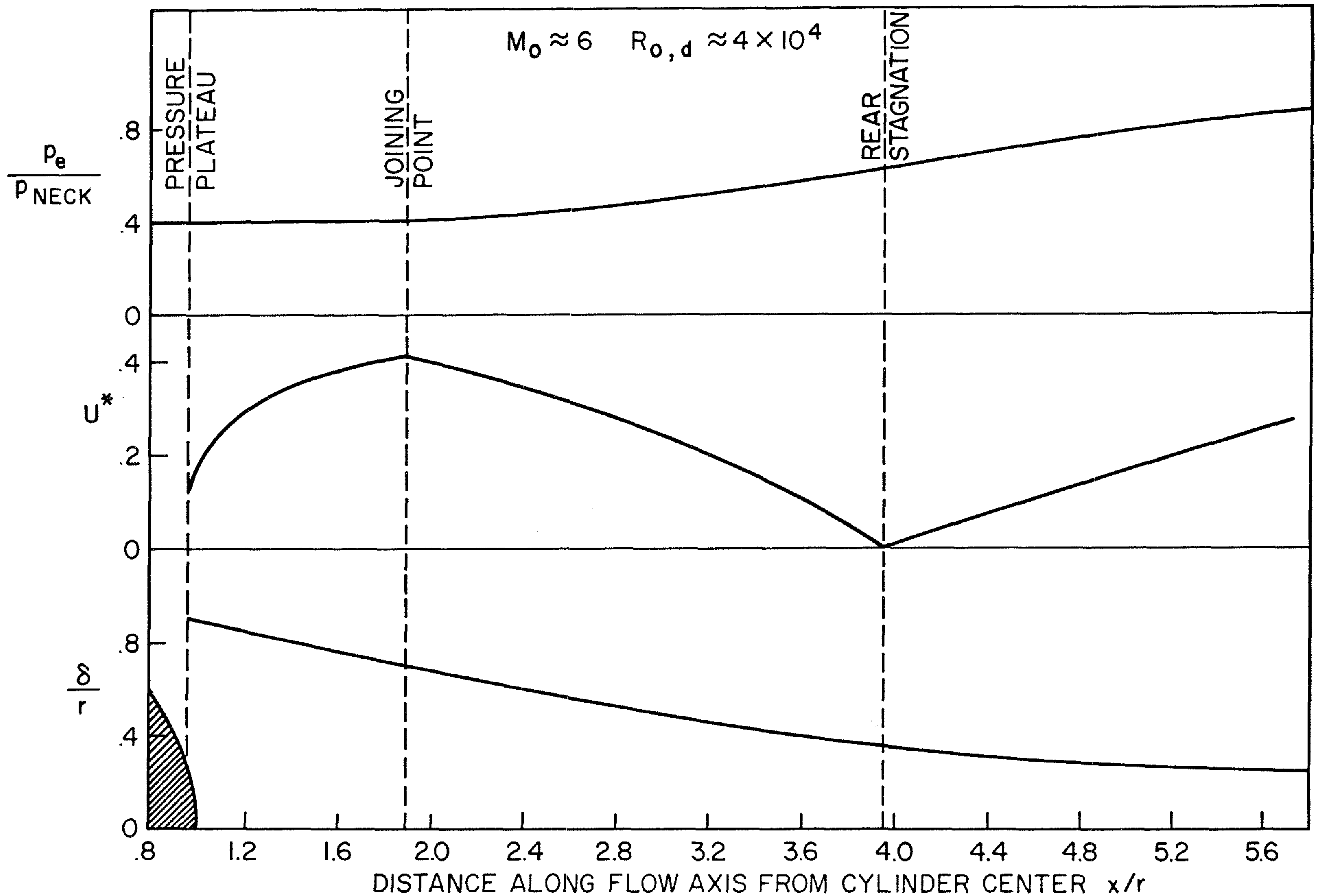

FIG. 15. NEAR WAKE INTERACTION REGION